Ontario

We are committed to providing accessible customer service.
If you need accessible formats or communications supports, please contact us.

Nous tenons à améliorer l’accessibilité des services à la clientèle.
Si vous avez besoin de formats accessibles ou d’aide à la communication, veuillez nous contacter.

Assessment Report

2021 Q1 Airborne Magnetic Survey

Q-Gold (Ontario) Ltd.

NTS Map Sheets 052/C10 - Bad Vermillion Lake Area (ENDM)

Rainy River District, ON

Patrick Lengyel, B. Sc., P. Geo

Winnipeg, MB, Canada

February 23, 2022

Table of Contents

Cover picture: drill set up at Foley Mine area May 2021

List of Figures

List of Tables

List of Appendices

Summary

The current report summarizes the results of an airborne magnetic survey completed on Q-Gold (Ontario) Ltd.'s Mine Centre project in the Mine Centre, ON area. The survey covered the entire land package that was in good standing in Q1 2021. A total of 2575 kilometers of data was collected from January 19th to January 30th, 2021.

Property Location, Access, and Tenure

General Location

The property is in the Rainy Lake District midway between the towns of Fort Frances and Atikokan, and immediately south of the community of Mine Centre, ON (Figure 1). The south end of the property is nearly contiguous with the eastern margin of Seine River First Nation Community 23B and is approximately 10 km west of Seine River First Nation Community 23A. The property straddles the Little Turtle Lake and Bad Vermillion Lake area townships, and NTS sheets 052/C15 and 052/C10. Most of the property covers the ground between Bad Vermillion Lake and Shoal Lake.

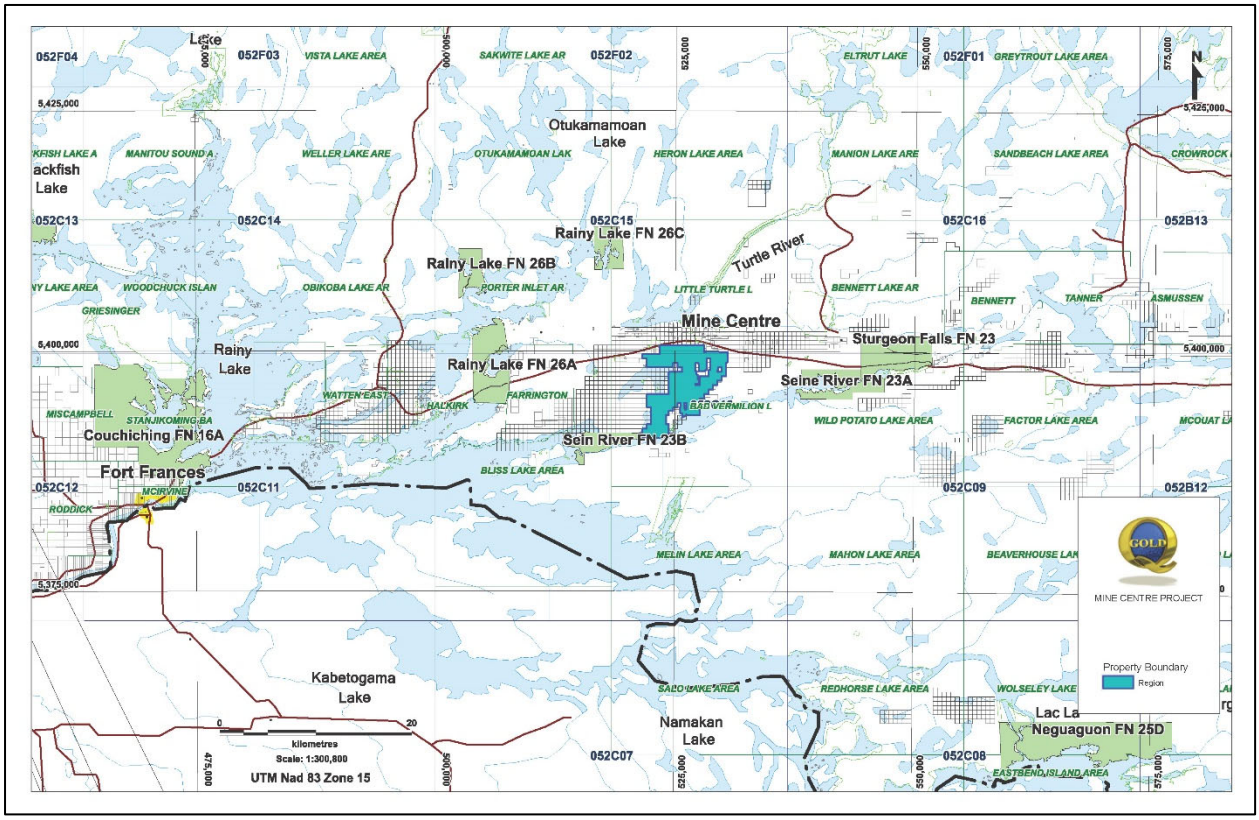

Figure 1 - General Location

Numerous cottages are present on the north and west shore of Bad Vermillion Lake, along the west shore of Shoal Lake. A former outfitter camp located at the confluence of Bad Vermillion River and the southwest end of Shoal Lake may have recently been purchased by Seine River First Nation interests.

Access

The property is road accessible via the west and east. From Winnipeg, MB, access is via TransCanada Highway 1, Ontario Provincial Highways 17, 71 and 11 over approximately 496 km. From Thunder Bay, ON, access is via Ontario Provincial Highways 17 and 11 over approximately 281 km. Access to the numerous showings between Bad Vermillion Lake and Shoal Lake can be gained via the all-weather Shoal Lake Road that extends approximately 25 km south from a turnoff on Provincial Highway 11 approximately 1.3 km east of Mine Centre to the confluence of Bad Vermillion River and Shoal Lake. Public lake access to Bad Vermillion Lake is available at Mine Centre and from a landing on the McKenzie Gray site. Shoal Lake can be accessed via a private landing on the southeast corner of Lease LEA-107790.

Tenure

At the time of the drilling program, the Mine Centre property comprised 3 mining patents, 7 mining leases, 152 single cell claims and 41 boundary cell claims totalling approximately 41 km^2 (Figure 2). The claim details are summarized in Appendix 1.

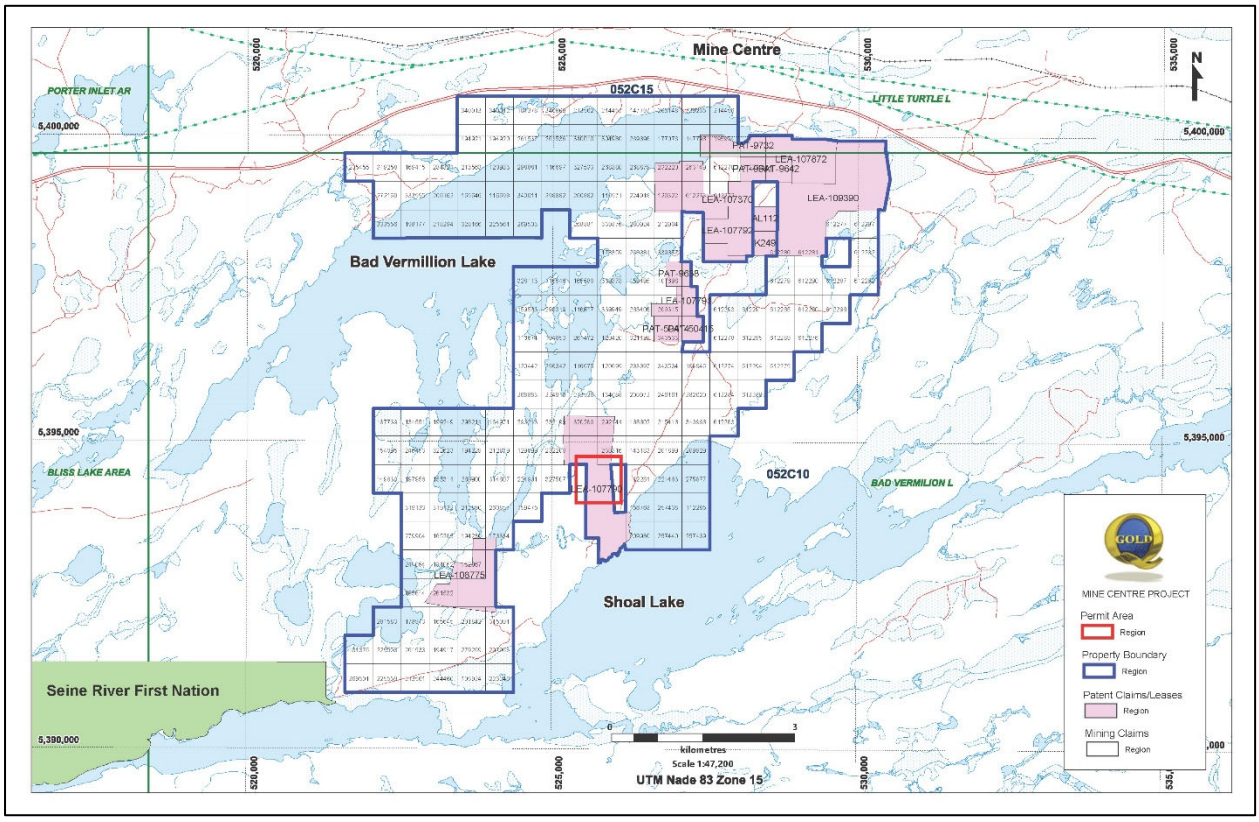

Figure 2 - Access & Tenure

Historical Work

General Location

The current property began with the acquisition of the northern half that was the subject of a 43-101 report (Northwest Mineral Development Services, 2006 & 2011) and was later expanded to the south to include Foley Mine and the McKenzie Gray showing areas (Tortosa, 2011, 2012).

Historically, gold was first discovered in the area in 1893 with two phases of development: 1893-1900 and 1920-1930. After 1940, exploration was sporadic. There are numerous exploratory shafts throughout the district, however, the only significant gold production came from the Foley (4,412 oz Au), Golden Star (10,758 oz Au) and Olive (3,654 oz Au) Mines. Recessions, forest fires and labour shortages also affected activity.

The most significant recent historic work prior to 1997 was completed by Sherritt Gordon Mines Ltd. who completed widespread surface geological mapping and sampling in 1982.

Hexagon Gold (Ontario) Ltd. acquired the property in 1997, completing several surface sampling programs from 1997-2000.

Q-Gold acquired the bulk of property from Hexagon Gold in 2005 and has performed a variety of geophysical, geological, diamond drilling and dewatering programs from 2005-present under two distinct management teams. Underground workings for Foley and Golden Star Mines were digitized during this period and based on the drilling reported here, the Foley Mine workings appear to be reasonably accurately located. The southern claims that cover the McKenzie Gray Prospect were acquired in 2007 from Nipigon Gold with subsequent work programs from 2009-2010. Q-Gold work programs were suspended in 2012 and activity resumed in September 2020 under the new management team.

Property Geology

General Setting

The Mine Centre property, located in the Rainy Lake Block of Ontario, is underlain by Neoarchean rocks of the Superior Province. The Rainy Lake Block is a fault-bounded region at the boundary between the

granite-greenstone Western Wabigoon terrane to the north and the Quetico sedimentary gneiss terrane to the south (Figure 3).

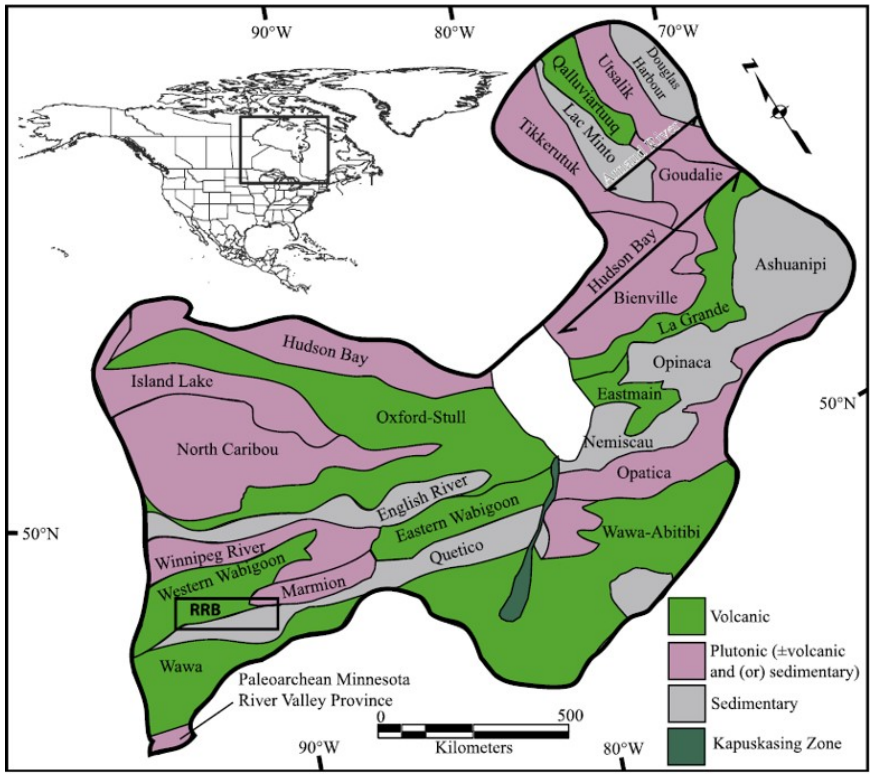

Figure 3-Superior Province

Rocks from both terranes occur within the fault-bounded region and are unconformably overlain by Timiskaming-type sediments of the Seine Group and intruded by post-peak metamorphism potassic Algoman granites (Poulsen, 2000).

Wabigoon terrane rocks include a variety of ultramafic to felsic volcanic rocks of Mg-tholeiite to Fe-tholeiite, tholeiite and calc-alkaline affinity with interbedded synvolcanic clastic and chemical sediments. The depositional environment was deep to shallow marine with local emergent edifices in ocean plateau and back arc rift settings from 2755-2695 Ma. All units are intruded by a range of synvolcanic, syn-metamorphic and post-peak metamorphic intrusions, including layered intrusions locally (e.g. Bad Vermillion Lake area). Metamorphic grade is primarily greenschists facies increasing locally to amphibolite facies adjacent to batholithic margins with peak metamorphism age ranges spanning 2467-2460 Ma. Late tectonic alkalic flows and volcaniclastics, broadly coeval Timiskaming-type sediments, and associated late tectonic intrusions, occur throughout the terrane (e.g. Cameron Lake and Stormy Lake areas). Unmetamorphosed intrusion dates span 2654-2485 Ma.

Quetico terrrane rocks are primarily turbiditic metasediments that grade from biotite schist in the north to migmatite in the south, that are open folded throughout with many of the antiforms cored by massive granitoid intrusions. Age dates from the sedimentary units and associated intrusions range from 2660-2625 Ma. Metamorphic grade increases from greenschist facies in the north to amphibolite facies in the south.

Rainy River Block rocks are primarily deformed volcanic and intrusive rocks from the south edge of the Wabigoon terrane with minor marine sediments along the southern margin that may be lower metamorphic grade equivalents from the Quetico terrane to the south. All are unconformably overlain by Seine River Group Timiskaming-type rocks (Figure 4: Units 3c & 3d; Figure 5) on the east end of the block.

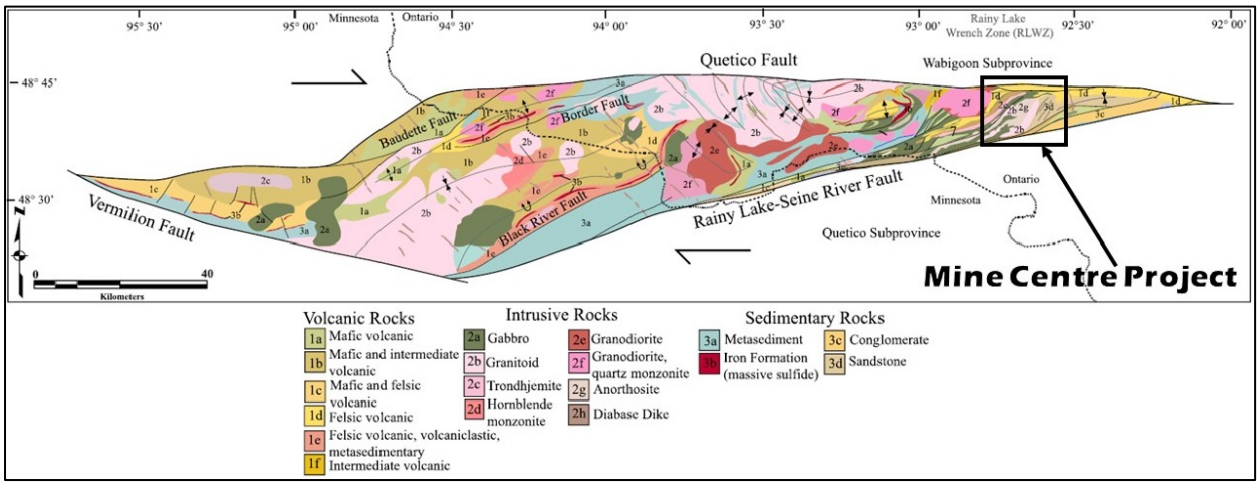

Figure 4-Rainy River Block Geology (modified from Hendrickson, 2016a)

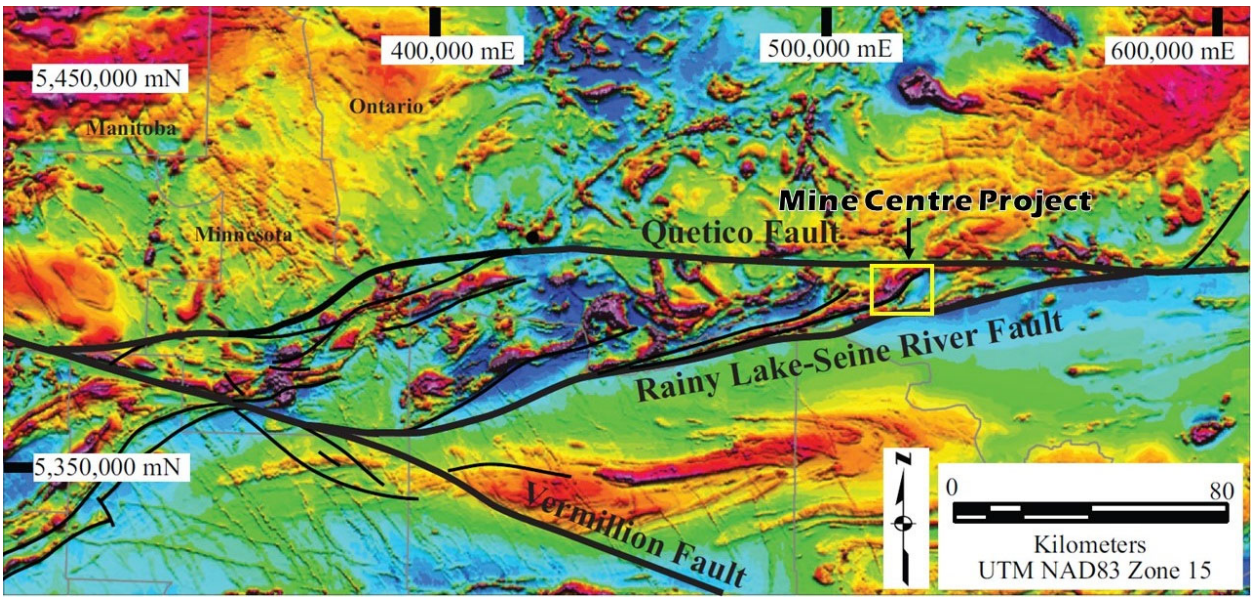

Figure 5-Rainy River Block (modified from Hendrickson, 2016b)

The Rainy River Block is a fault-bounded assemblage with the highest strain rocks, referred to as the Rainy Lake Wrench Zone, located in the eastern end. The dominant structural feature is the Rainy Lake-Seine River fault, which separates this section of the Western Wabigoon from the Quetico terrane to the south. The fault has a sharp contact with the Quetico sediments, can be as narrow as 50 m, and is composed primarily of chlorite schist and phyllonite. Kinematic indicators indicate a dextral sense of displacement. The Quetico Fault, in contrast, is a zone up to 1 km wide of intensely foliated rocks

containing mylonite and local pseudotachylite. The fault truncates the late tectonic Ottertail Lake pluton, indicating that it formed relatively late in the structural evolution of the block.

Internally, the Rainy River Block contains numerous fault- or discontinuity-bounded domains, each containing up to 3.5 km of accumulated stratigraphy that cannot be correlated from one block to the other (Figure 6) suggesting a relatively complex structural history. The Mine Centre project straddles the Bad Vermillion and Mine Centre blocks.

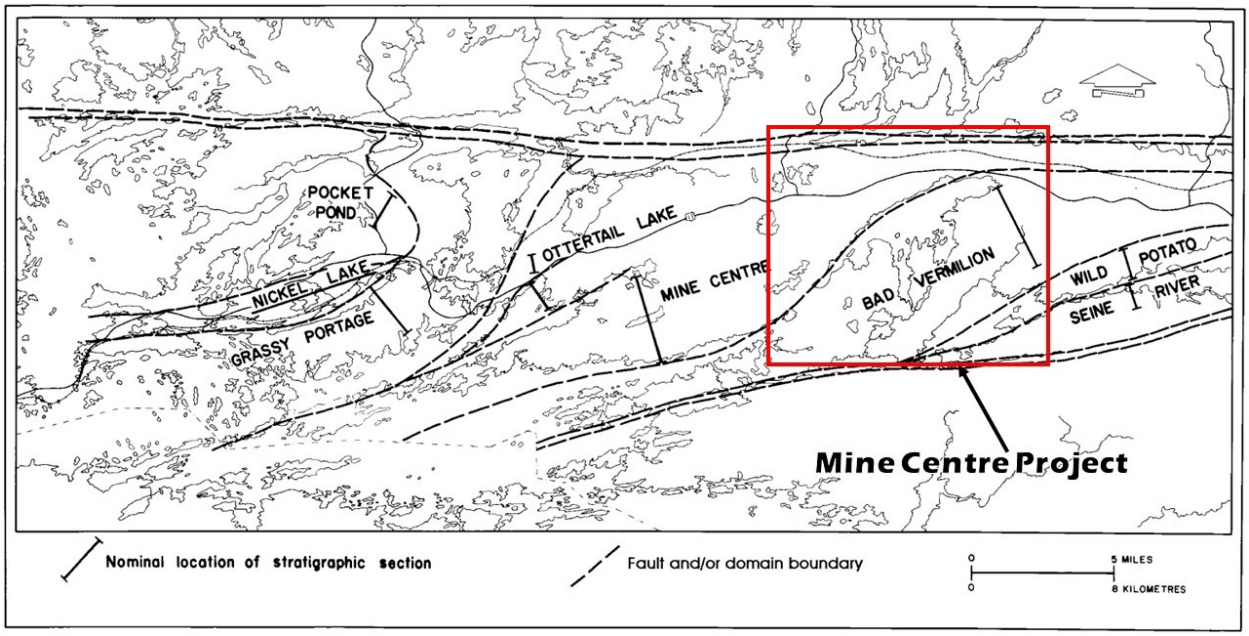

Figure 6-East Rainy River Block domains (modified from Poulsen 2000)

A simplified geology map (Figure 7) illustrates the main geological assemblages in the property area. The Mine Centre block stratigraphy is primarily intermediate to felsic volcanic flows and volcaniclastics intruded by a significant number of mafic, synvolcanic sills. Bad Vermillion block stratigraphy includes a bimodal sequence of mafic and felsic volcanics. A syn-volcanic (?) bimodal gabbro-tonalite/trondhjemite intrusive complex intrudes both blocks. The Ottertail intrusion is located west of the Mine Centre block and its northern edge is truncated by the Quetico fault. Most of the volcanic and intrusive rocks are overlain by the Timiskaming-type Seine River Group shallow marine to subaerial arkosic sandstones and conglomerate.

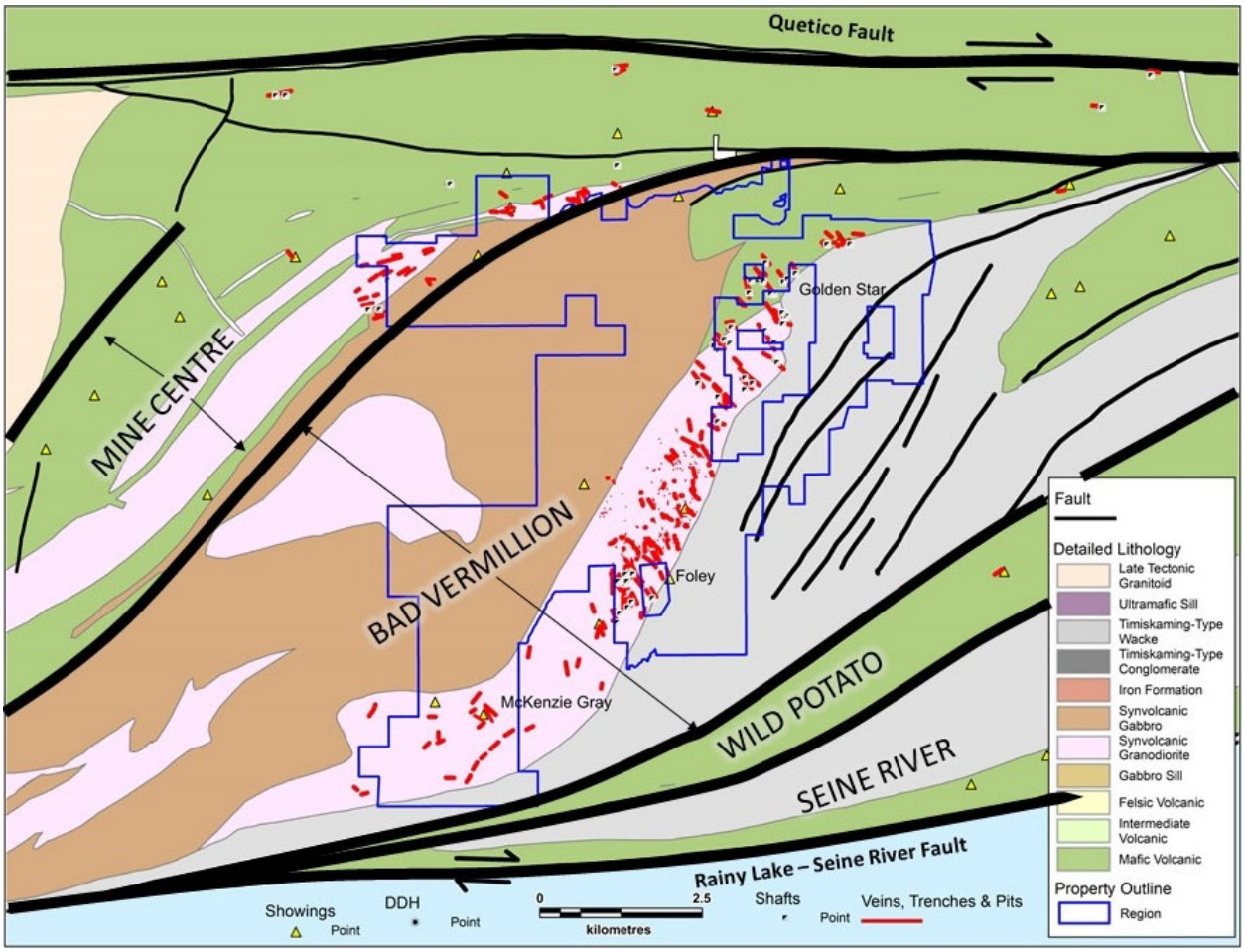

Figure 7 - Property Geology

The structural geology is typical for Archean greenstone belts with at least one early and likely non-penetrative phase associated with early thrust faulting and recumbent folding. Vestiges of the early deformation are preserved as opposite directed tops in otherwise homogeneous panels. The Rainy Lake-Seine River fault, a major terrane bounding discontinuity, would have been active during early thrusting. Thrust vergence is assumed to be in a northerly direction but the absolute direction is not preserved. Subsequent northwest directed shortening resulted in the dominant features preserved in the belt, including the 060 Az trending foliation throughout the Wabigoon and Quetico terranes. The Rainy Lake-Seine River Fault remained the dominant feature, although with continued shortening the Quetico fault formed, and continued shortening resulted in the formation of numerous internal northeast-trending faults between the two in the form a regional wrench fault system.

Poulsen (2000) identified the major fault systems within the wrench fault system (Figure 8), which are all late tectonic in origin and consequently will contain most of the orogenic gold mineralization. North-northwest- and west-trending conjugate faults identified by Poulsen are the main structural features within the property. For example, mineralization at Foley Mine is largely controlled by north-northwest oriented shear zones while mineralization at McKenzie-Gray is largely controlled by West-trending shear zones. These orientations also shift depending on any post-faulting rotation within the wrench fault system.

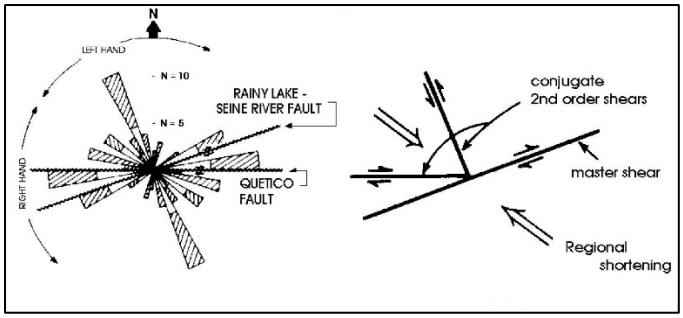

Figure 8-modified from Poulsen (2000) Figures 14b & 14c

2021 Q1 Airborne Magnetic Survey

Overview

The 2021 Q1 airborne magnetic survey was completed by Scott Hogg & Associates from January 19th to January 30th, 2021. The survey was carried out with an A-Star 350D helicopter towing a Heli-GT three-axis magnetic gradiometer over a survey grid with 50-meter spaced lines and 30 meter terrane clearance. A variety of magnetic features were produced from the survey data as well as a digital terrain model. A detailed technical report of the survey is included in Appendix 2.

Survey Products

Survey products include grd and jpg outputs of the following:

1. Total Magnetic Intensity (TMI), useful for mapping out main lithologies

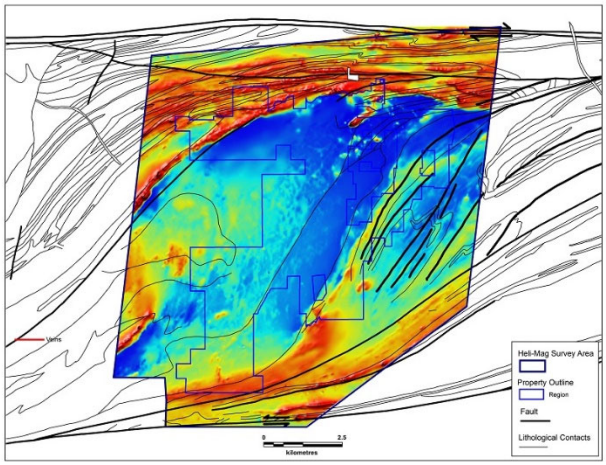

Figure 9 TMI

2. Total Magnetic Intensity Reduced to Pole (TMIRTP), more accurately locates anomalies by compensating for the angle of the magnetic field

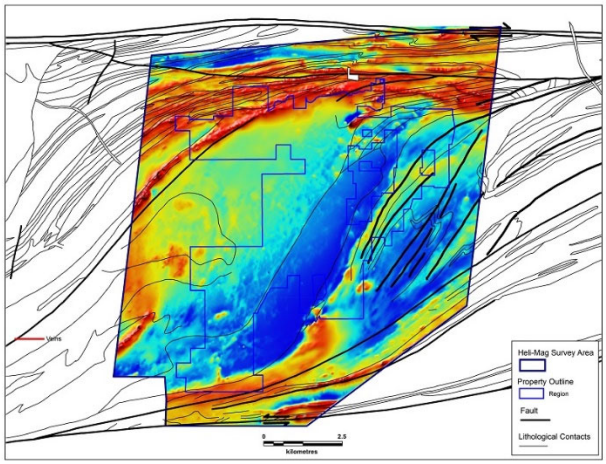

Figure 10 TMIRTP

3. Analytical Signal (ANS), reflects proximity to the source and can be useful for mapping out small features such as trend lines and also vertical offsets.

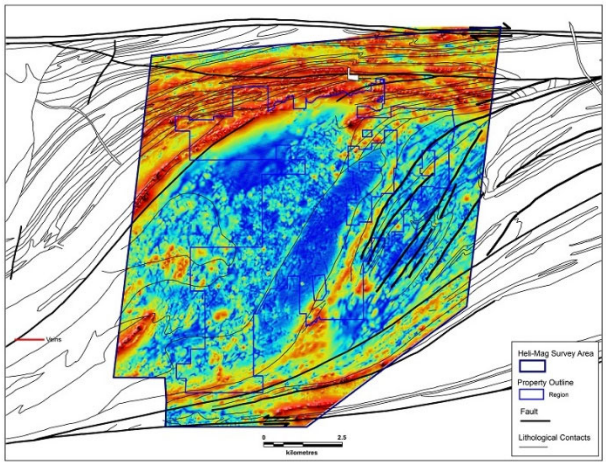

Figure 11 ANS

4. Horizontal Gradient (HGrad), useful for mapping out geological contacts.

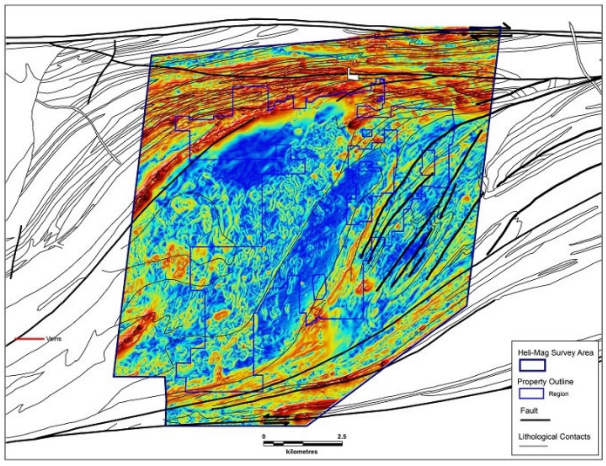

Figure 12 HGrad

5. Tilt Derivative (Tdrv), useful for resolving weak or complex magnetic anomalies.

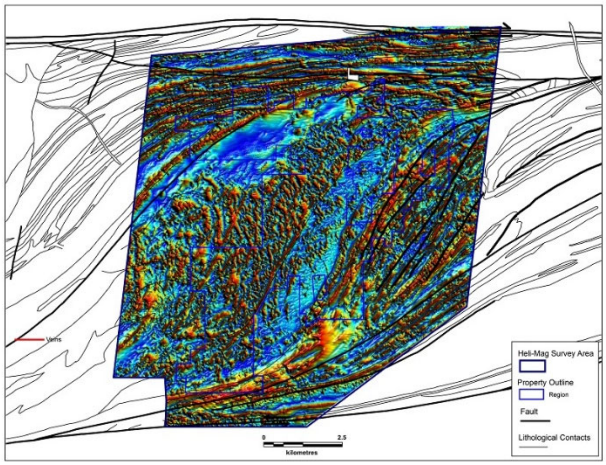

Figure 13 Tdrv

6. First Vertical Gradient Reduce to Pole (CVGRTP), useful for mapping out major units or magnetic regions and structures

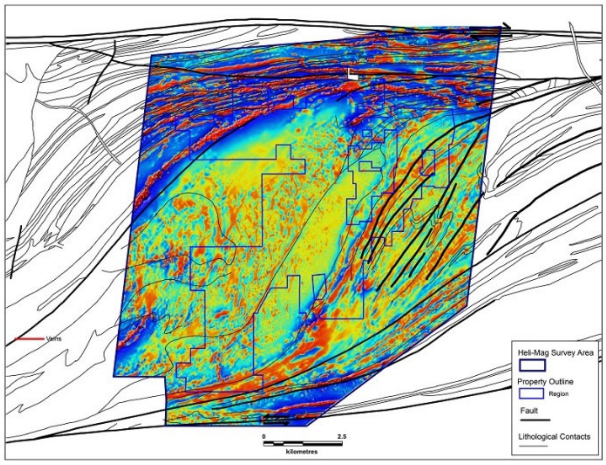

Figure 14 CVGRTP

7. Second Vertical Gradient Reduced to Pole (2VGRTP), useful for mapping out smaller scale features.

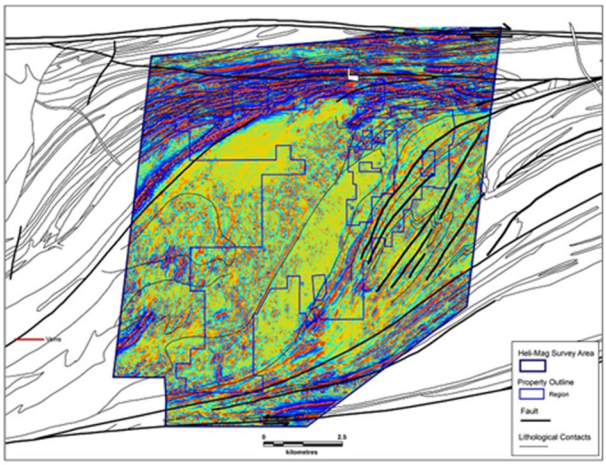

Figure 15 2VGRTP

8. Digital Terrain Model (DTM), useful for mapping out lithology and structure.

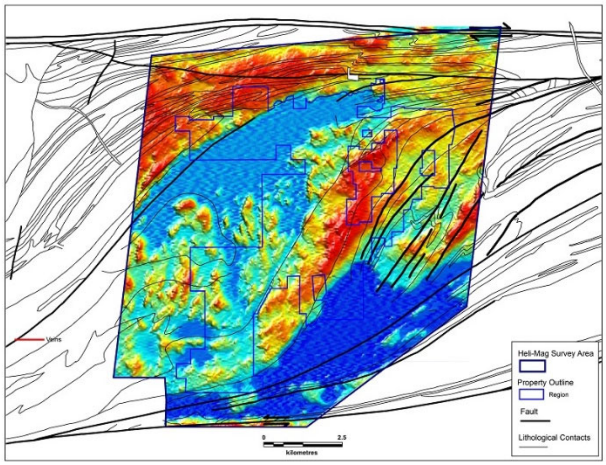

Figure 16 DTM

The above map products have been included with the filed assessment report as separate pdf format products.

Magnetic Data Interpretation

Major Lithology

A plot of TMIRTP vs basic lithologies (Figure 17) highlights a variety of magnetic responses. Synvoclanic tonalite sills (Unit A), found on the west and east sides of Bad Vermillion Lake, have a relatively low magnetic signature that appears to increase towards the south. The increase in magnetic signature could be due to an increase in metamorphic grade towards the Quetico terrane, or it could be due to a transition towards more mafic composition.

Synvolcanic gabbro sills (Unit B), the dominant lithology in the synvolcanic layered intrusion centered on Bad Vermillion Lake, also becomes more magnetic towards the south. The magnetic shift could be due to metamorphic grade or a compositional shift towards, perhaps, a feeder conduit.

Synvolcanic iron formations (Unit C) occur in several of the assemblages but it is unclear whether the composition is sulphide or oxide.

Residual Fe-Ti-V mineralization (Unit D), hosted by gabbroic layers in the layered synvolcanic sill complex, has previously been identified on the western margin of the survey area. Similar responses within the gabbro in the southwest boundary of the survey area (D?) may be an extension of the same style of mineralization.

Previously mapped alternating units of intermediate to felsic volcanics and thin, synvolcanic gabbro sills in the northwest end of the survey area (Unit F) are not in good agreement with the aeromagnetic data. The latter suggests a significantly higher number of sills are present and the overall deformation appears to be more complex.

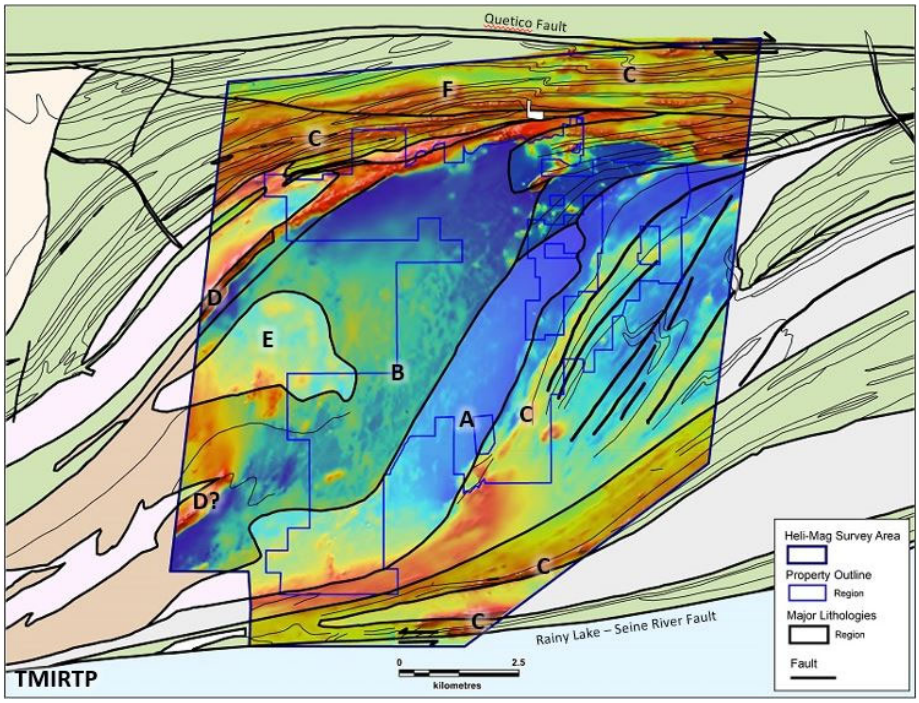

Figure 17 - TMIRTP with basic lighologies (A=tonalite, B=synvolcanic gabbro, C=synvolcanic iron formation, D=residual Fe-Ti-V in gabbro, E=synvolcanic felsic intrusion, F=alternating synvocanic gabbro sills and felsic-int volcanics)

In addition to mapping out basic lithologies, the survey may have identified non-outcropping felsic late tectonic intrusions. In Figure 18, two magnetic low areas stand out in the tilt derivative plot. Both occur beneath lakes and do not appear to outcrop, so the composition is unknown, however, the low magnetic response is similar to the known late tectonic intrusion on the northwest margin of the figure.

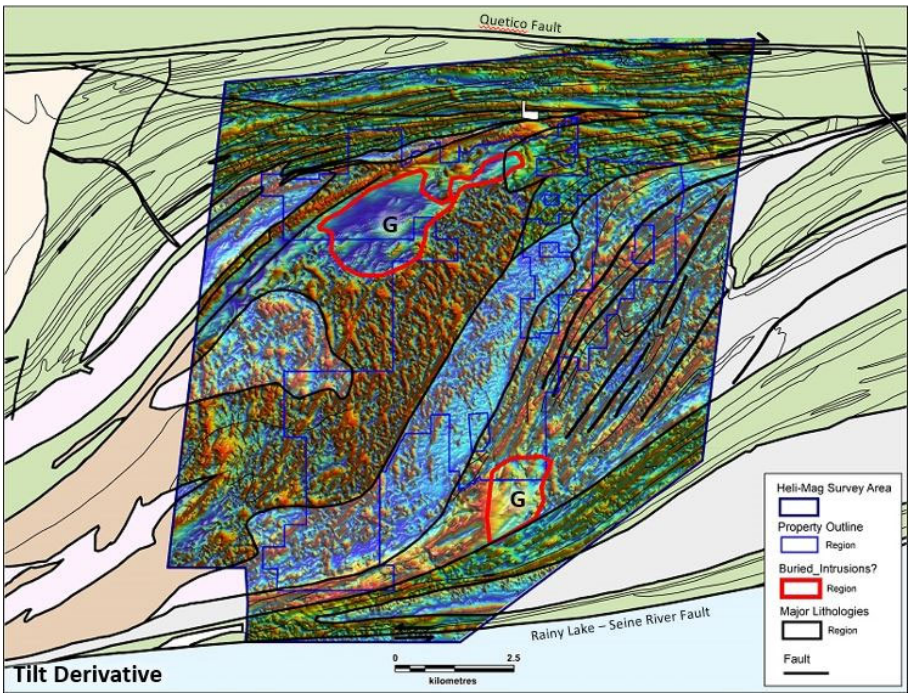

Figure 18 - Tilt Derivative with major lithologic boundaries and possible buried late tectonic intrusions

Structure

The 2021 magnetic data is the first survey to have adequate resolution to detect the abundant 2nd order structures first reported by Poulsen. Vertical gradient data (Figure 19) shows many north-northwest and West-Southwest trending linear features in the filtered magnetic data demarcated by arrows. The linear features are subparallel with Poulsen's mapped structures and in many cases correspond with known bedrock faults, mineralization, or extensions of it along strike. It is unclear whether the linear features represent vertical offsets in primary lithology or magnetic dykes intruding faults, however, it would not be unexpected to have late tectonic mafic dykes (e.g. lamprophyre) being emplaced along conjugate faults throughout the survey area.

Detailed structural interpretations are also possible using the 2021 magnetic data. A photo of an outcrop approximately 25m north of Foley Shaft (Figure 20) shows an abundance of faults and fractures in the granodiorite host rock that conform to Poulsen's 2nd order shear zones. The majority of the mineralization at Foley Mine is hosted by north-trending faults that are subparallel to the features in the outcrop. Similar outcrop-scale features at McKenzie-Gray are in agreement with west-trending features in the magnetic data there. What is unclear is the importance of the offsets observed in outcrop and what role, if any, they may play in the continuity of structures and mineralization at the deposit and property scale.

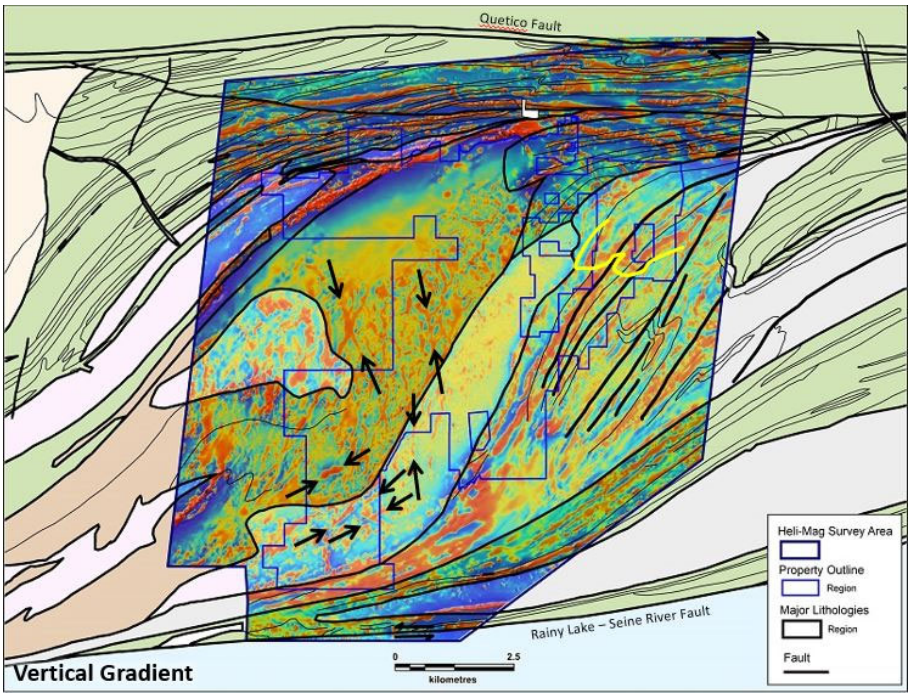

Figure 19 - Vertical Gradient Data with major lithologic boundaries and arrows demarkating linear magnetic features along faults

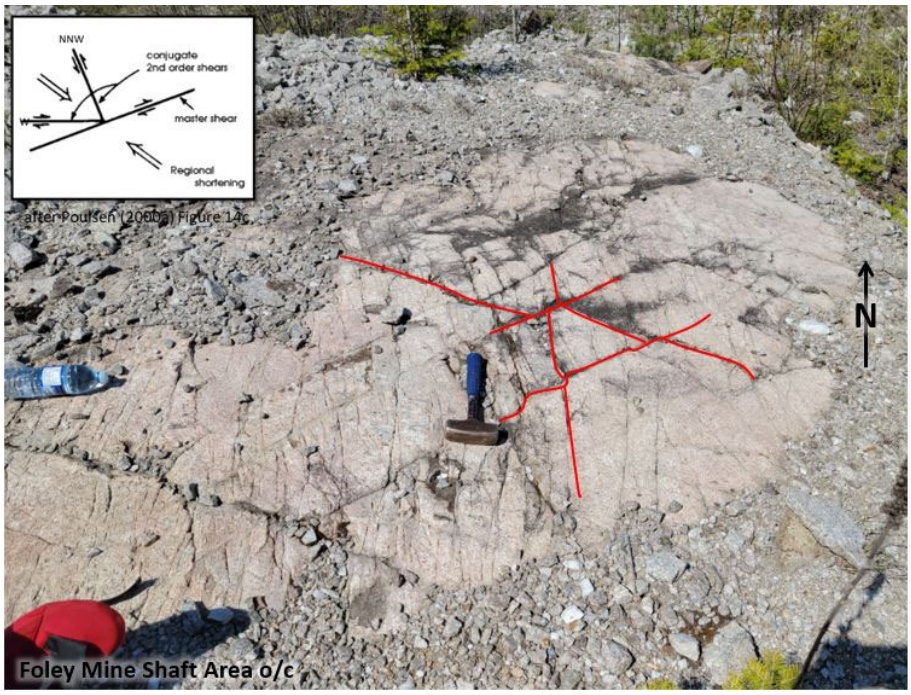

Figure 20 - Foley Mine Outcrop

A detailed interpretation was completed using all the geophysical products generated by the 2021 survey, with significant reliance on the analytical signal, 1st and 2nd vertical derivatives, tilt derivative and horizontal gradient (Figure 21).

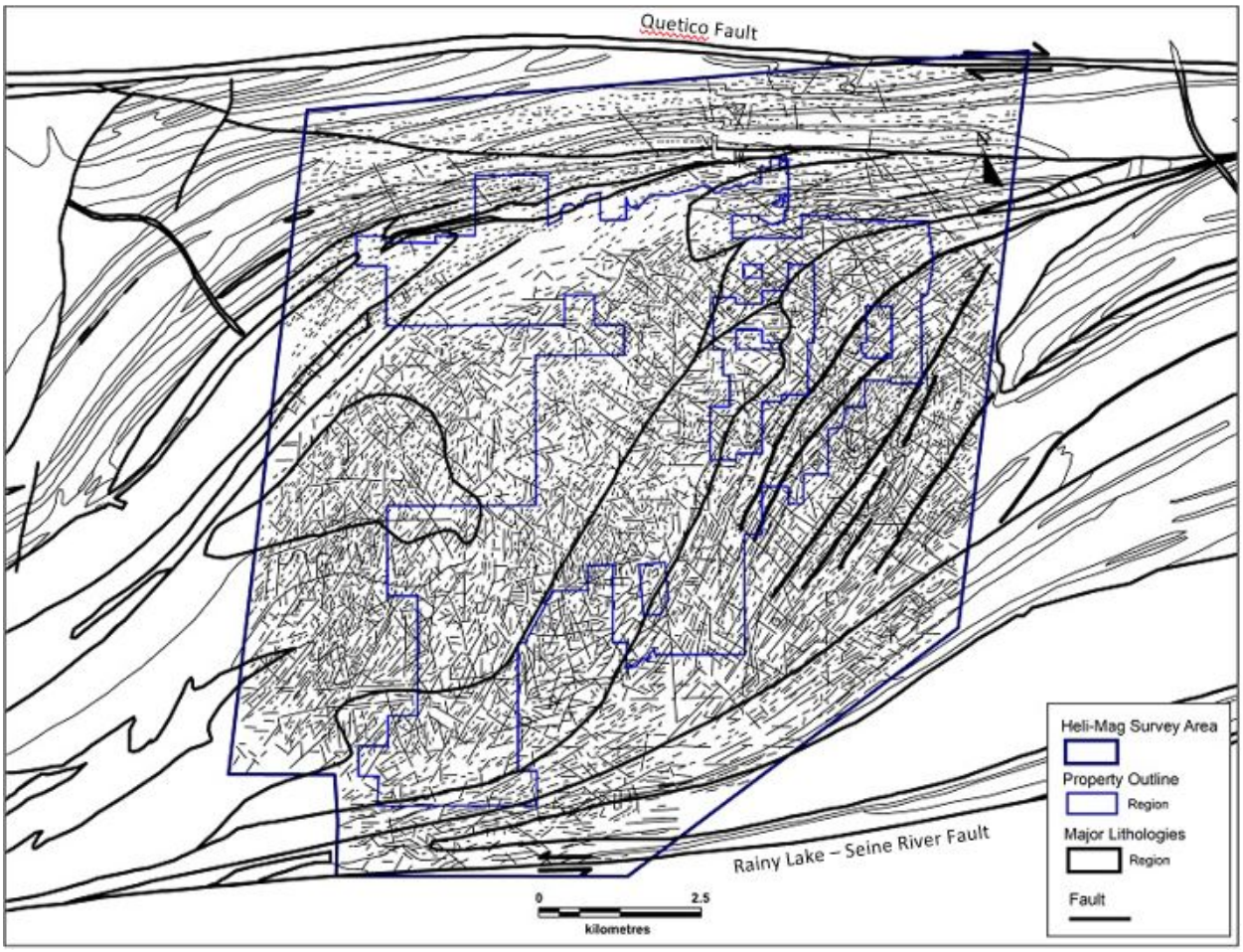

Figure 21-Interpreted Structures from Magnetic Data

The interpreted data indicates that there are an exceptionally high number of 2nd order shear zones/faults within the bimodal synvolcanic intrusive complex that conform to Poulsen's interpreted north to north-northwest and west to west-southwest orientations. There also appears to be a third set of northwest oriented features that are subparallel to the interpreted shortening direction, but these could also be extension features related to sinistral rotation within the wrench fault system.

Figures 22, 23 & 24 are plots of the direction-specific features shown cumulatively in Figure 21. In each case, known historic mineralization occurs on several of the interpreted faults, including the northwest-oriented faults that are one of Poulsen's main second order (conjugate) shear orientations.

Although preliminary, it does appear that there may be a rough 1-2 km spacing to what might be main 2nd order shear zones, with abundant smaller faults and fractures between them.

In addition to geological features, it should be noted that several of the historic shafts have small circular magnetic responses. Given the amount of old equipment on several of the sites off the current property, it is likely that there are additional cultural anomalies.

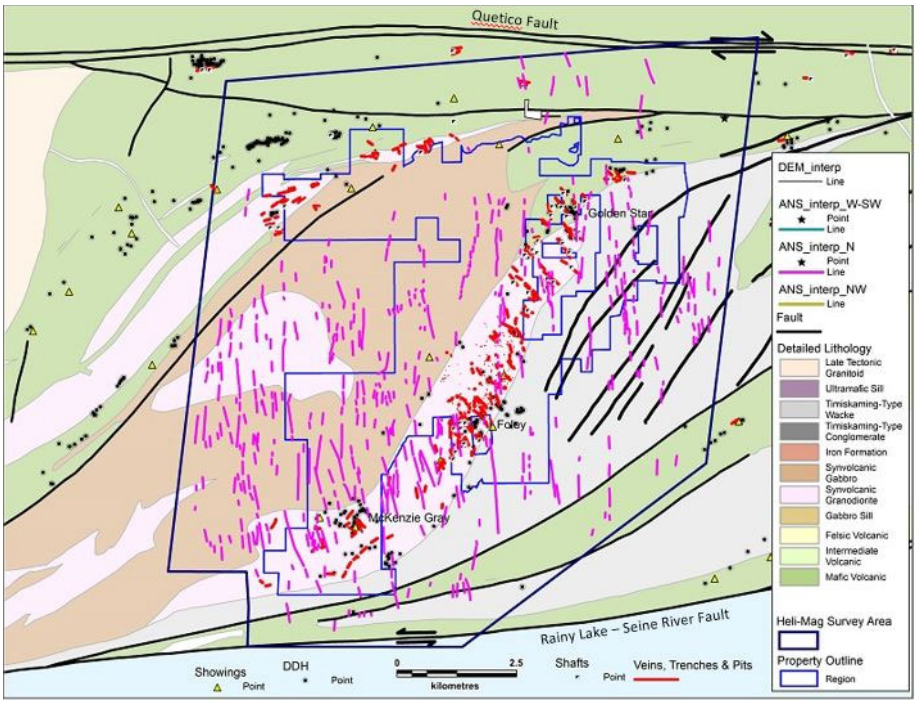

Figure 22 - north-trending interpreted faults from magnetic data

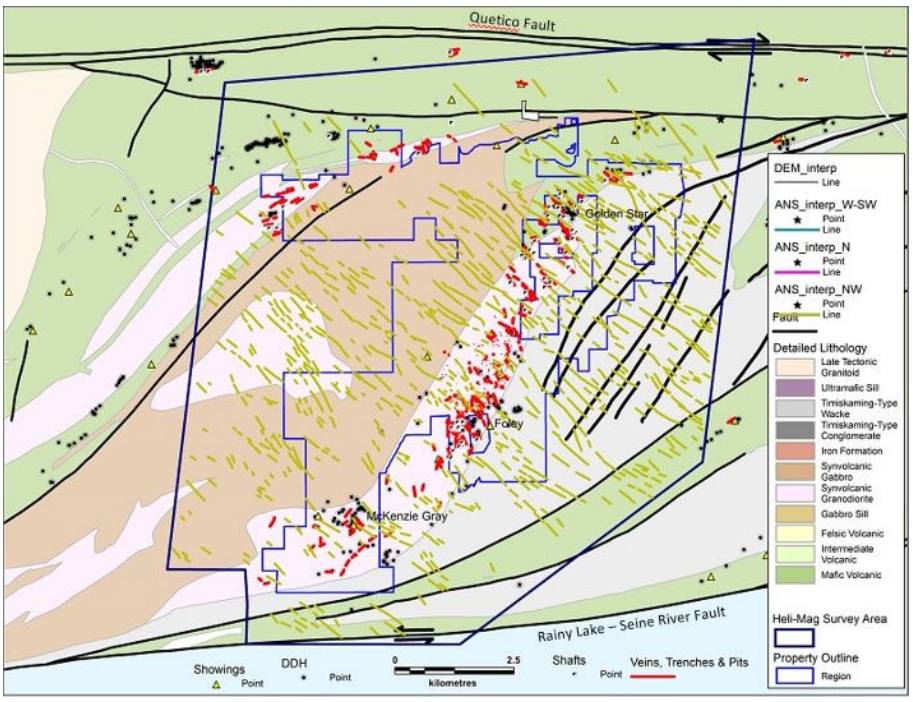

Figure 23 - northwest trending interpreted faults from magnetic data

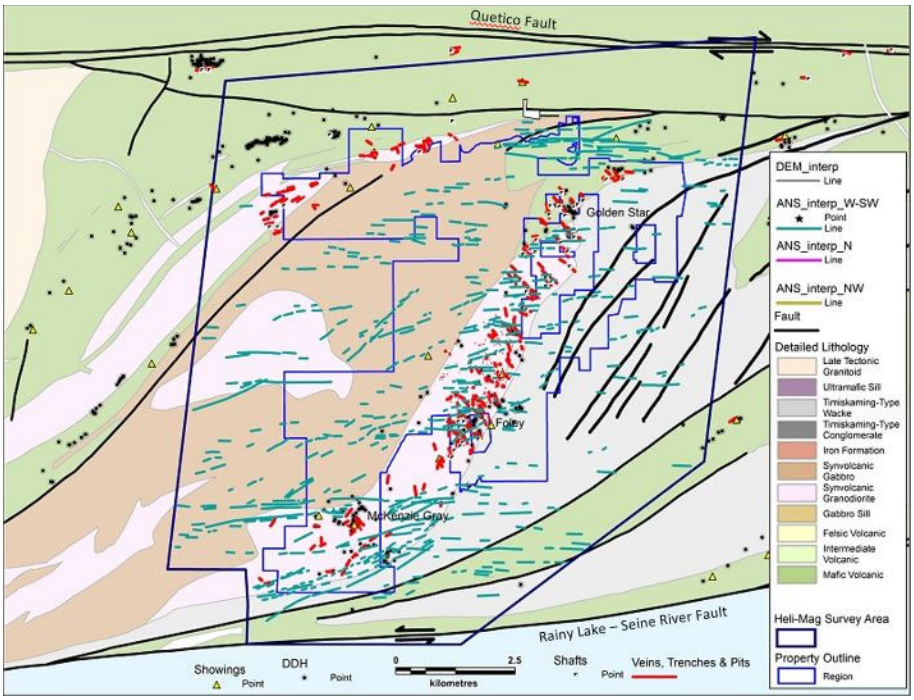

Figure 24 - west trending interpreted faults from magnetic data

In addition to the property scale features above, linear magnetic anomalies/interpreted faults are also observed at the showing scale. In Figure 25, a variety of features can be observed at the showing scale. In the Foley Mine area, magnetic high features can represent magnetite-rich beds in Timiskaming sediment (Feature A) or igneous flow banding (Feature B). Magnetic low areas can be the dipolar interstices between magnetic highs (Feature C), zones of magnetite destruction along structures (Feature D), or offsets of magnetic highs that occur from horizontal and/or vertical displacement (Feature E). Linear magnetic features occur coincident with known veins (Feature F) and as linear features that extend along strike from existing veins (Feature G between arrows).

The main shaft at Foley Mine, which was refurbished in the last decade, stands out as a small but strong, circular high (Feature H). The older shafts, which remain largely untouched from their development approximately 100 years ago, do not have magnetic high responses.

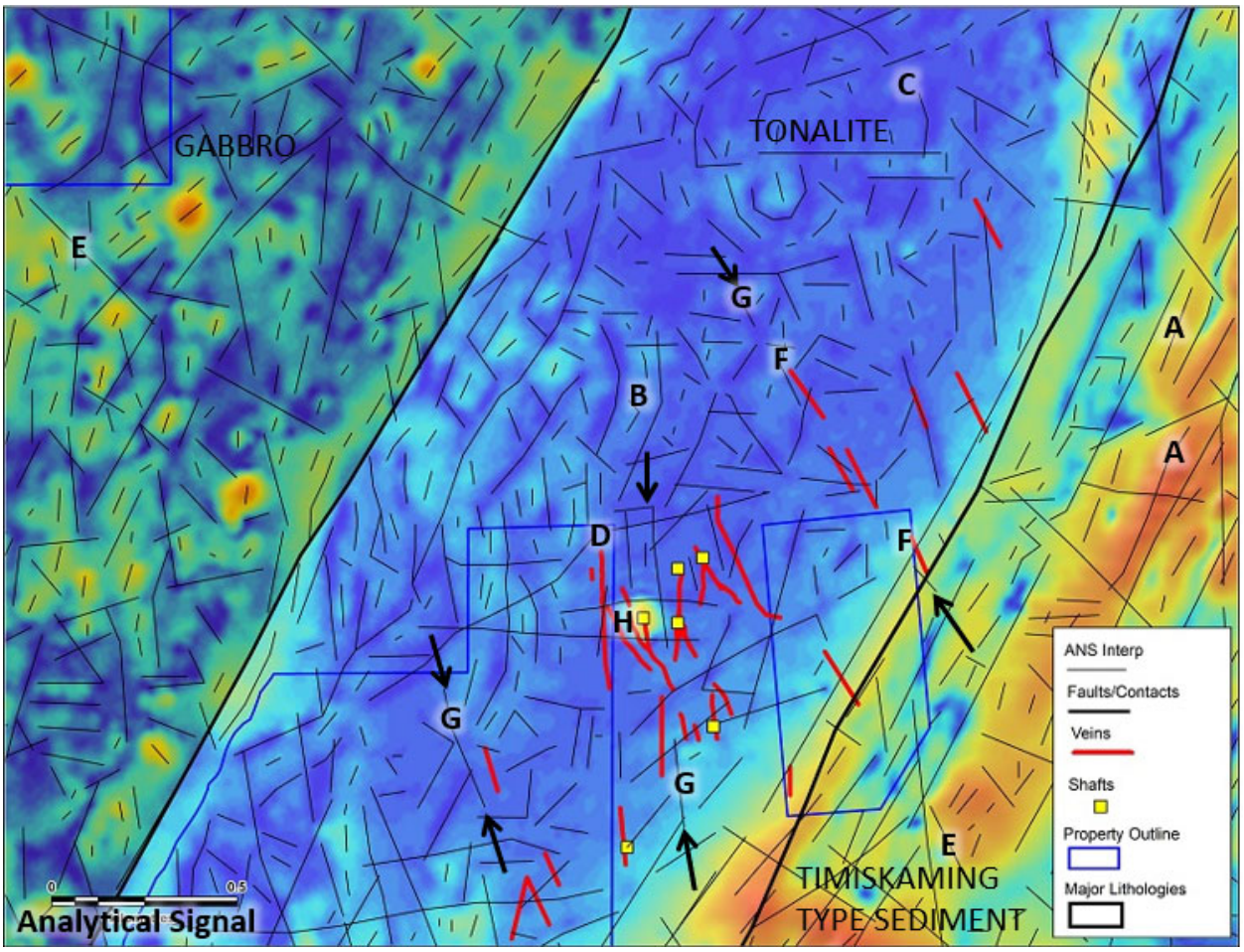

Figure 25 – magnetic-derived interpreted faults in the Foley Mine area (A=magnetic high lithologies, B=potential intrusive flow banding, C=magnetic low interstices, D=magnetic destruction along shear zones, E=faulted offsets of magnetic highs, F=interpreted faults associated with known mineralization, G=interpreted faults along strike from, or subparallel to, existing mineralization, H=Foley Mine shaft magnetic high)

DTM Data Interpretation

In addition to magnetic data, the 2021 survey also collected elevation data with the radar altimeter and GPS that was used to produce a digital terrain model (DTM). Although this data is ineffective where there is significant overburden like lakes and wetlands, and its best responses are from lithologies that are more prone to deformation and are topographic highs, it is still very valuable data.

Major Lithologies

Figure 26 is a colour contour plot of the DTM elevation data. While there is some alignment with major lithologies, it is far less obvious than what is observed in magnetic data due to erosion and overburden cover.

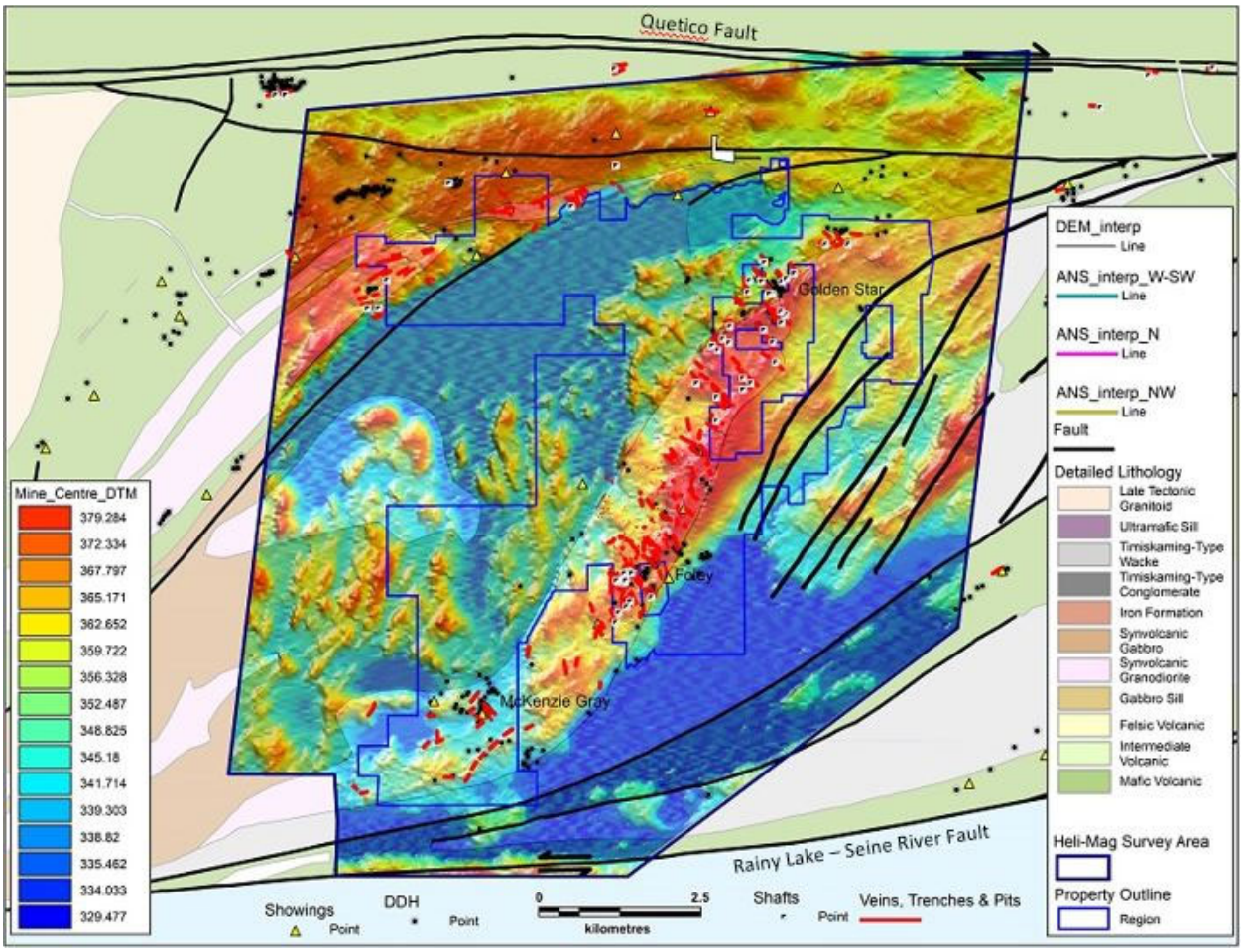

Figure 26 - 2021 DTM

Structure

Although relatively poor for major lithology interpretation, DTM data is very useful for interpretation structure, and in the case of the 2021 survey, corroborating magnetic interpretations. Figure 26, and the structures interpreted from the DTM data in Figure 27, show that the majority of the historic gold showings occur on linear topographic features, and that many appear to have significant strike extensions. Unfortunately, DTM products derived from radar altimeter have a modest resolution of approximately 30 m. A LiDAR survey would provide higher resolution data in the order of 10 cm that could, in theory, be followed at the outcrop scale.

A close up of the Foley Mine area in Figure 28 shows that even relatively course DTM data is useful at the showing scale. The colour contour base shows the elevation data with thicker dark blue lines representing interpreted faults. Thin black lines are the interpreted magnetic features. Many of the structures interpreted from DTM data coincide with known vein arrays and with interpreted magnetic features and extend along strike from many.

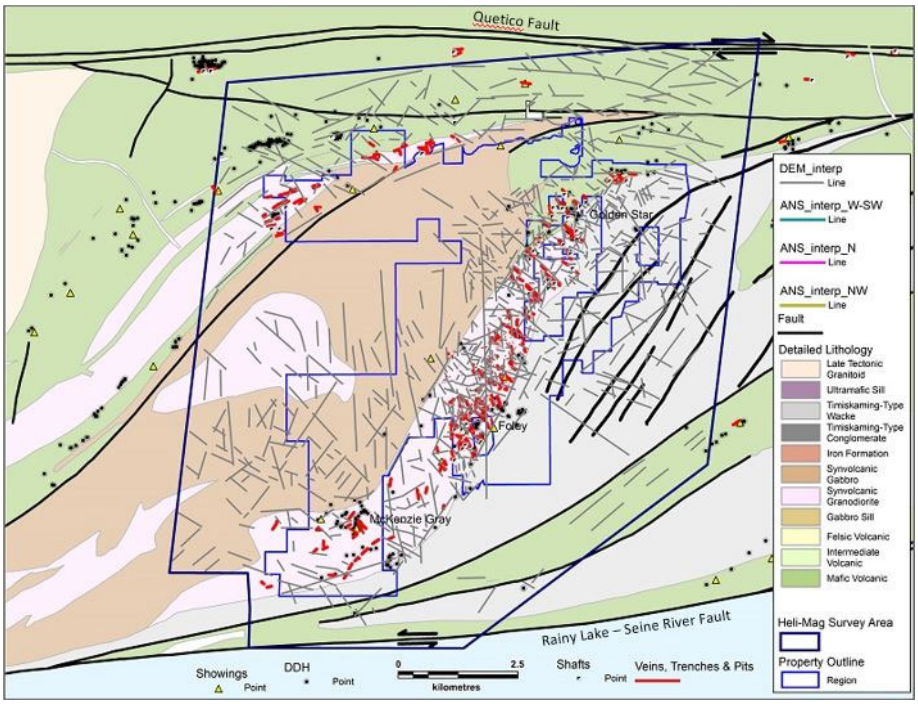

Figure 27 - Interpreted structures from DTM

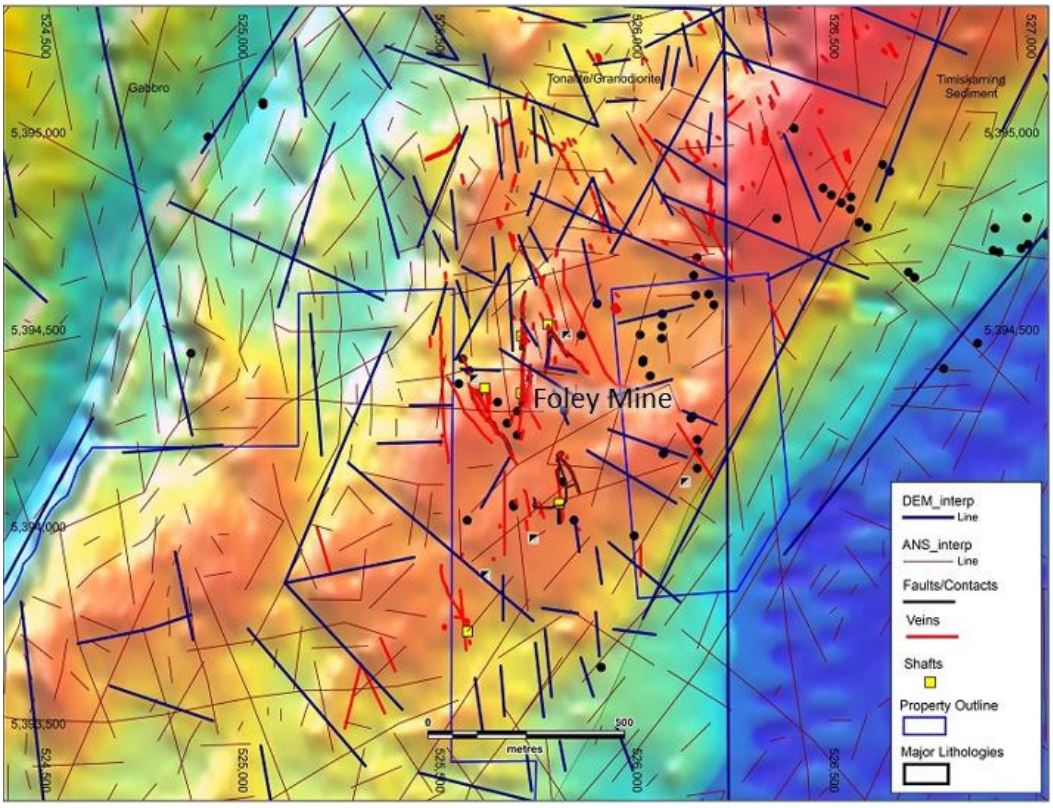

Figure 28 - DTM interpreted structures overlain on interpreted magnetic features, Foley Mine area

Other Airborne Products

A 3D magnetic inversion model was generated using the 2021 survey data. This product has the potential to highlight structures at depth, structural interpretation in general, and also help identify buried features such as late tectonic intrusions. Further work with this data is recommended as the property evolves.

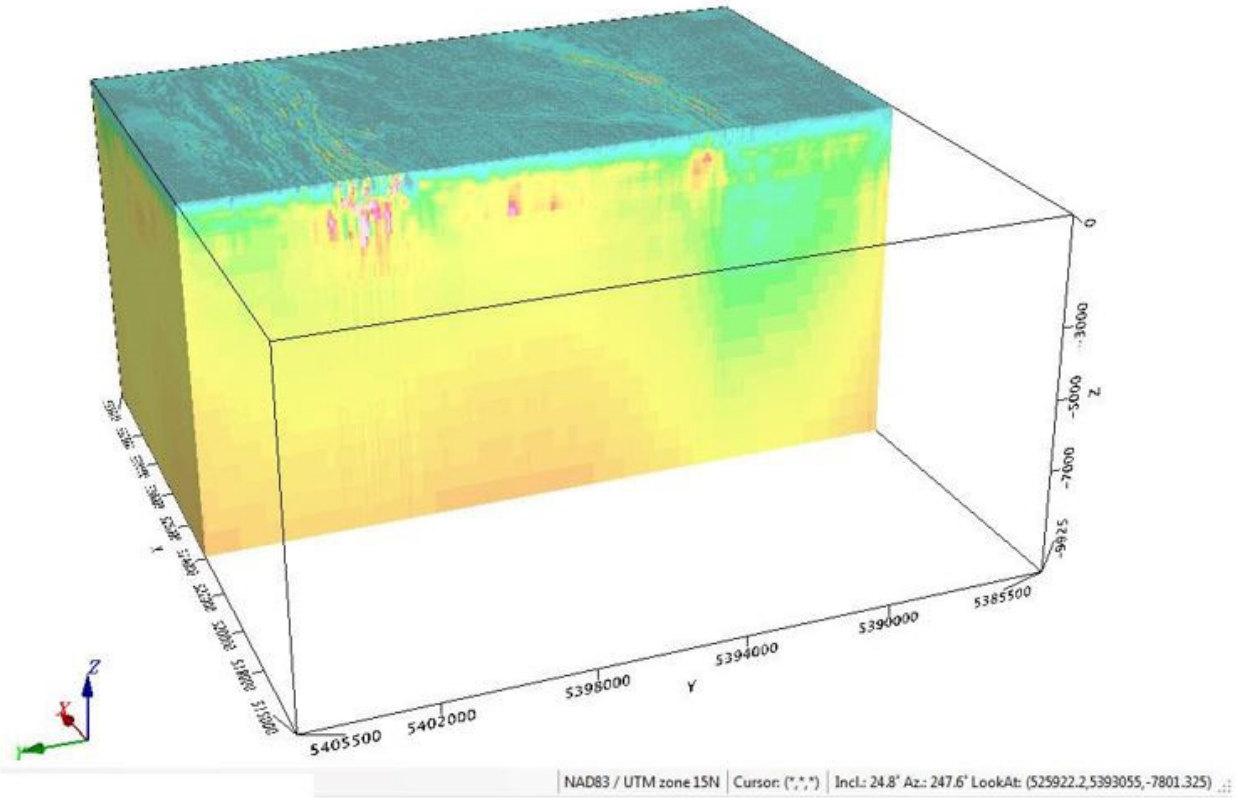

Figure 29-3D Magnetic Inversion Model

Although the expenditures were not included in the current assessment report filing, the contractor also completed a review of two recent airborne electromagnetic surveys and the results are in the corporate files. Although conductive overburden dominates the responses, there were what appear to be significant bedrock conductors in the data as well.

Conclusions

The 2021 airborne magnetic survey substantially upgraded the bedrock magnetic data for the project, providing high resolution data based on 50m spaced lines with optimal terrain clearance on the helicopter platform.

Although one of the main host lithologies, the granodiorite stock that hosts the Foley Mine, has a relatively low magnetic response, the data still proved to be extremely useful in defining linear features in the magnetic data that coincide with historic occurrences and provide abundant exploration targets along strike.

Although the DTM data from the survey is relatively course compared to the magnetic data, it showed remarkable coincidence with historic showings and mapped faults and provided abundant exploration targets along strike.

Recommendations

It is recommended that the interpreted products from the 2021 airborne survey be incorporated into a comprehensive exploration program that includes:

1. A high-resolution LiDAR survey
2. follow up property-wide surface exploration program that includes updated mapping and geochemical sampling,
3. follow up showing-specific, and reconnaissance drill programs, based on the results of the above work

References

Beard, R. 2006. Report for Q-Gold Resources, Limited On the Northwestern Ontario Gold & Base Metal Properties, Mine Centre Area, Rainy River District, FormallyHeld by Hexagon Gold (Ontario) Limited, 159p.

2011. Technical Report for Cadman Resources Inc. On the Golden Star, Baseline and Nugget Vein Gold Property, Mine Centre Area, Kenora District, Ontario, 157p.

Hendrickson, M.D. 2016a. Geologic interpretation of aeromagnetic and chemical data from Oaks Belt, Wabigoon subprovince, Minnesota: implications for Au-rich VMS deposit exploration, Can. J. Earth Sci, 53: p.176-188.

2016b. Structural analysis of aeromagnetic data from the Rainy River Block, Wabigoon subprovince, Minnesota, USA and Ontario, Canada: Strain partitioning along a Neoarchean terrane boundary and implications for mineral exploration, Precambrian Research 286, p. 20-34.

Tortosa, D. 2011. Report on the 2010 Diamond Drilling Program, Foley Mine Property, Mine Centre Property, Kenora District, Ontario for Q-Gold Resources Limited, 38p.

2012. Report on the 2011 Diamond Drilling Program, McKenzie Gray Prospect, Nipigon Area Property, Mine Centre, Kenora District, Ontario for Q-Gold Resources Limited, 31 p.

Poulsen, H. 2000. Archean Metallogeny of the Mine Centre-Fort Frances Area, Ontario Geological Survey, Report 266, 121 p.

Certificate of Qualifications

I, J.W. Patrick Lengyel, am a Professional Geoscientist, retained by Q-Gold Resources Ltd, and by extension, its subsidiary, Q-Gold (Ontario) Ltd., of Toronto, Ontario, and declare that:

1. I graduated from the University of Manitoba with a Bachelor of Science degree in Geological Sciences (Honours) in 1988.
2. I am a registered Professional Geoscientist in good standing with the Association of Professional Geoscientists of Ontario (#0420), Engineers and Geoscientists Manitoba (#20259), and the Association of Professional Engineers and Geoscientists of Saskatchewan (#11384).
3. I have worked continuously as a Geologist since graduation, primarily on gold, base metal and industrial mineral properties in North and South America and Africa.
4. I have been managing the Q-Gold Mine Centre project continuously since August 28th, 2020.
5. I supervised the work described in this report.
6. I am the author of this report.

Dated at Winnipeg, Manitoba, on 23rd of February, 2022.

_____

J.W. Patrick Lengyel, B. Sc., P. Geo.

Appendix 1 – Claim Table & Figures

Table 1 - Claim List

Legacy Claim Id	Township / Area	Tenure ID	Tenure Type	Anniversary Date	Tenure Status	Tenure Percentage
3000810	LITTLE TURTLE LAKE AREA	340013	Boundary Cell Mining Claim	24-Feb-22	Active	100
3000810	LITTLE TURTLE LAKE AREA	340012	Boundary Cell Mining Claim	24-Feb-22	Active	100
3000810	BAD VERMILION LAKE AREA	340011	Boundary Cell Mining Claim	24-Feb-22	Active	100
3000810	BAD VERMILION LAKE AREA	269503	Boundary Cell Mining Claim	24-Feb-22	Active	100
3000810	BAD VERMILION LAKE AREA	225561	Boundary Cell Mining Claim	24-Feb-22	Active	100
3000810	LITTLE TURTLE LAKE AREA	194921	Boundary Cell Mining Claim	24-Feb-22	Active	100
3000810	LITTLE TURTLE LAKE AREA	101378	Boundary Cell Mining Claim	24-Feb-22	Active	100
3000810	BAD VERMILION LAKE AREA,LITTLE TURTLE LAKE AREA	298881	Single Cell Mining Claim	24-Feb-22	Active	100
3000810	LITTLE TURTLE LAKE AREA	261537	Single Cell Mining Claim	24-Feb-22	Active	100
3000810	LITTLE TURTLE LAKE AREA	194920	Single Cell Mining Claim	24-Feb-22	Active	100
3000810	BAD VERMILION LAKE AREA,LITTLE TURTLE LAKE AREA	120983	Single Cell Mining Claim	24-Feb-22	Active	100
3000810	BAD VERMILION LAKE AREA	116698	Single Cell Mining Claim	24-Feb-22	Active	100
3000811	BAD VERMILION LAKE AREA	298882	Boundary Cell Mining Claim	24-Feb-22	Active	100
3000811	LITTLE TURTLE LAKE AREA	340010	Single Cell Mining Claim	24-Feb-22	Active	100
3000811	LITTLE TURTLE LAKE AREA	340009	Single Cell Mining Claim	24-Feb-22	Active	100
3000811	LITTLE TURTLE LAKE AREA	261536	Single Cell Mining Claim	24-Feb-22	Active	100
3000811	LITTLE TURTLE LAKE AREA	213562	Single Cell Mining Claim	24-Feb-22	Active	100
3000811	BAD VERMILION LAKE AREA,LITTLE TURTLE LAKE AREA	116697	Single Cell Mining Claim	24-Feb-22	Active	100
3000812	LITTLE TURTLE LAKE AREA	304980	Single Cell Mining Claim	24-Feb-22	Active	100
3000813	LITTLE TURTLE LAKE AREA	339235	Single Cell Mining Claim	24-Feb-22	Active	100
3000813	LITTLE TURTLE LAKE AREA	269896	Single Cell Mining Claim	24-Feb-22	Active	100
3000813	BAD VERMILION LAKE AREA,LITTLE TURTLE LAKE AREA	263149	Single Cell Mining Claim	24-Feb-22	Active	100
3000813	LITTLE TURTLE LAKE AREA	263148	Single Cell Mining Claim	24-Feb-22	Active	100
3000813	LITTLE TURTLE LAKE AREA	214457	Single Cell Mining Claim	24-Feb-22	Active	100
3000813	LITTLE TURTLE LAKE AREA	214456	Single Cell Mining Claim	24-Feb-22	Active	100
3000813	LITTLE TURTLE LAKE AREA	195924	Single Cell Mining Claim	24-Feb-22	Active	100
3000813	LITTLE TURTLE LAKE AREA	177076	Single Cell Mining Claim	24-Feb-22	Active	100
3000813	LITTLE TURTLE LAKE AREA	147798	Single Cell Mining Claim	24-Feb-22	Active	100
3000813	LITTLE TURTLE LAKE AREA	147797	Single Cell Mining Claim	24-Feb-22	Active	100
3000811	BAD VERMILION LAKE AREA	260882	Boundary Cell Mining Claim	28-Mar-22	Active	100
3000811	BAD VERMILION LAKE AREA,LITTLE TURTLE LAKE AREA	327533	Single Cell Mining Claim	28-Mar-22	Active	100
3000812	BAD VERMILION LAKE AREA,LITTLE TURTLE LAKE AREA	268880	Single Cell Mining Claim	28-Mar-22	Active	100
3000813	BAD VERMILION LAKE AREA,LITTLE TURTLE LAKE AREA	268879	Single Cell Mining Claim	28-Mar-22	Active	100
3000813	BAD VERMILION LAKE AREA,LITTLE TURTLE LAKE AREA	232220	Single Cell Mining Claim	28-Mar-22	Active	100
3000814	BAD VERMILION LAKE AREA	281583	Boundary Cell Mining Claim	28-Mar-22	Active	100
3000814	BAD VERMILION LAKE AREA	225558	Boundary Cell Mining Claim	28-Mar-22	Active	100
3000814	BAD VERMILION LAKE AREA	101376	Boundary Cell Mining Claim	28-Mar-22	Active	100
3000814	BAD VERMILION LAKE AREA	269501	Single Cell Mining Claim	28-Mar-22	Active	100
3000814	BAD VERMILION LAKE AREA	261532	Single Cell Mining Claim	28-Mar-22	Active	100
3000814	BAD VERMILION LAKE AREA	225559	Single Cell Mining Claim	28-Mar-22	Active	100
3000814	BAD VERMILION LAKE AREA	178973	Single Cell Mining Claim	28-Mar-22	Active	100
3000814	BAD VERMILION LAKE AREA	165645	Single Cell Mining Claim	28-Mar-22	Active	100
3000814	BAD VERMILION LAKE AREA	165644	Single Cell Mining Claim	28-Mar-22	Active	100
3000815	BAD VERMILION LAKE AREA	279904	Single Cell Mining Claim	28-Mar-22	Active	100
3000815	BAD VERMILION LAKE AREA	244054	Single Cell Mining Claim	28-Mar-22	Active	100
3000815	BAD VERMILION LAKE AREA	184062	Single Cell Mining Claim	28-Mar-22	Active	100
3000815	BAD VERMILION LAKE AREA	165285	Single Cell Mining Claim	28-Mar-22	Active	100
3000815	BAD VERMILION LAKE AREA	132067	Single Cell Mining Claim	28-Mar-22	Active	100
3000816	BAD VERMILION LAKE AREA	199249	Boundary Cell Mining Claim	28-Mar-22	Active	100
3000816	BAD VERMILION LAKE AREA	187739	Boundary Cell Mining Claim	28-Mar-22	Active	100
3000816	BAD VERMILION LAKE AREA	154095	Boundary Cell Mining Claim	28-Mar-22	Active	100
3000816	BAD VERMILION LAKE AREA	149830	Boundary Cell Mining Claim	28-Mar-22	Active	100
3000816	BAD VERMILION LAKE AREA	134551	Boundary Cell Mining Claim	28-Mar-22	Active	100

3000816	BAD VERMILION LAKE AREA	322623	Single Cell Mining Claim	28-Mar-22	Active	100
3000816	BAD VERMILION LAKE AREA	319133	Single Cell Mining Claim	28-Mar-22	Active	100
3000816	BAD VERMILION LAKE AREA	319132	Single Cell Mining Claim	28-Mar-22	Active	100
3000816	BAD VERMILION LAKE AREA	246453	Single Cell Mining Claim	28-Mar-22	Active	100
3000816	BAD VERMILION LAKE AREA	197956	Single Cell Mining Claim	28-Mar-22	Active	100
3000816	BAD VERMILION LAKE AREA	153314	Single Cell Mining Claim	28-Mar-22	Active	100
3000817	BAD VERMILION LAKE AREA	328113	Boundary Cell Mining Claim	28-Mar-22	Active	100
3000817	BAD VERMILION LAKE AREA	165580	Boundary Cell Mining Claim	28-Mar-22	Active	100
3000817	BAD VERMILION LAKE AREA	159583	Boundary Cell Mining Claim	28-Mar-22	Active	100
3000817	BAD VERMILION LAKE AREA	120442	Boundary Cell Mining Claim	28-Mar-22	Active	100
3000817	BAD VERMILION LAKE AREA	116674	Boundary Cell Mining Claim	28-Mar-22	Active	100
3000817	BAD VERMILION LAKE AREA	116646	Boundary Cell Mining Claim	28-Mar-22	Active	100
3000817	BAD VERMILION LAKE AREA	298342	Single Cell Mining Claim	28-Mar-22	Active	100
3000817	BAD VERMILION LAKE AREA	298319	Single Cell Mining Claim	28-Mar-22	Active	100
3000817	BAD VERMILION LAKE AREA	261472	Single Cell Mining Claim	28-Mar-22	Active	100
3000817	BAD VERMILION LAKE AREA	194853	Single Cell Mining Claim	28-Mar-22	Active	100
3000817	BAD VERMILION LAKE AREA	116675	Single Cell Mining Claim	28-Mar-22	Active	100
3000817	BAD VERMILION LAKE AREA	116647	Single Cell Mining Claim	28-Mar-22	Active	100
3000820	BAD VERMILION LAKE AREA	268881	Boundary Cell Mining Claim	28-Mar-22	Active	100
3000820	BAD VERMILION LAKE AREA	224918	Single Cell Mining Claim	28-Mar-22	Active	100
3000820	BAD VERMILION LAKE AREA	120322	Single Cell Mining Claim	28-Mar-22	Active	100
3000820	BAD VERMILION LAKE AREA	116571	Single Cell Mining Claim	28-Mar-22	Active	100
3000815	BAD VERMILION LAKE AREA	194230	Single Cell Mining Claim	14-Jun-22	Active	100
3000816	BAD VERMILION LAKE AREA	298214	Boundary Cell Mining Claim	14-Jun-22	Active	100
3000816	BAD VERMILION LAKE AREA	280900	Single Cell Mining Claim	14-Jun-22	Active	100
3000816	BAD VERMILION LAKE AREA	212880	Single Cell Mining Claim	14-Jun-22	Active	100
3000816	BAD VERMILION LAKE AREA	194229	Single Cell Mining Claim	14-Jun-22	Active	100
3014617	BAD VERMILION LAKE AREA	164971	Boundary Cell Mining Claim	14-Jun-22	Active	100
3014617	BAD VERMILION LAKE AREA	327507	Single Cell Mining Claim	14-Jun-22	Active	100
3014617	BAD VERMILION LAKE AREA	314807	Single Cell Mining Claim	14-Jun-22	Active	100
3014617	BAD VERMILION LAKE AREA	260857	Single Cell Mining Claim	14-Jun-22	Active	100
3014617	BAD VERMILION LAKE AREA	232200	Single Cell Mining Claim	14-Jun-22	Active	100
3014617	BAD VERMILION LAKE AREA	224901	Single Cell Mining Claim	14-Jun-22	Active	100
3014617	BAD VERMILION LAKE AREA	212879	Single Cell Mining Claim	14-Jun-22	Active	100
3014617	BAD VERMILION LAKE AREA	178334	Single Cell Mining Claim	14-Jun-22	Active	100
3014617	BAD VERMILION LAKE AREA	159475	Single Cell Mining Claim	14-Jun-22	Active	100
3014617	BAD VERMILION LAKE AREA	129699	Single Cell Mining Claim	14-Jun-22	Active	100
4212912	BAD VERMILION LAKE AREA	107698	Single Cell Mining Claim	21-Jun-22	Active	100
3000814	BAD VERMILION LAKE AREA	261533	Single Cell Mining Claim	24-Jun-22	Active	100
3000814	BAD VERMILION LAKE AREA	213561	Single Cell Mining Claim	24-Jun-22	Active	100
3000814	BAD VERMILION LAKE AREA	194917	Single Cell Mining Claim	24-Jun-22	Active	100
855731	BAD VERMILION LAKE AREA	244460	Single Cell Mining Claim	24-Jun-22	Active	100
3000817	BAD VERMILION LAKE AREA	339949	Single Cell Mining Claim	9-Jul-22	Active	100
3000817	BAD VERMILION LAKE AREA	120420	Single Cell Mining Claim	9-Jul-22	Active	100
4212911	BAD VERMILION LAKE AREA	321129	Single Cell Mining Claim	9-Jul-22	Active	100
4212912	BAD VERMILION LAKE AREA	283406	Single Cell Mining Claim	9-Jul-22	Active	100
4212912	BAD VERMILION LAKE AREA	200315	Single Cell Mining Claim	9-Jul-22	Active	100
855740	BAD VERMILION LAKE AREA	120699	Single Cell Mining Claim	9-Jul-22	Active	100
855741	BAD VERMILION LAKE AREA	134088	Single Cell Mining Claim	9-Jul-22	Active	100
855742	BAD VERMILION LAKE AREA	292144	Single Cell Mining Claim	9-Jul-22	Active	100
875517	BAD VERMILION LAKE AREA	200972	Single Cell Mining Claim	9-Jul-22	Active	100
875543	BAD VERMILION LAKE AREA	246161	Single Cell Mining Claim	9-Jul-22	Active	100
875544	BAD VERMILION LAKE AREA	282020	Single Cell Mining Claim	9-Jul-22	Active	100
875544	BAD VERMILION LAKE AREA	184946	Single Cell Mining Claim	9-Jul-22	Active	100
875548	BAD VERMILION LAKE AREA	188802	Single Cell Mining Claim	9-Jul-22	Active	100
875550	BAD VERMILION LAKE AREA	230816	Single Cell Mining Claim	9-Jul-22	Active	100
875550	BAD VERMILION LAKE AREA	143183	Single Cell Mining Claim	9-Jul-22	Active	100
3000817	BAD VERMILION LAKE AREA	268883	Boundary Cell Mining Claim	18-Jul-22	Active	100
3000817	BAD VERMILION LAKE AREA	224919	Single Cell Mining Claim	18-Jul-22	Active	100
3000817	BAD VERMILION LAKE AREA	213526	Single Cell Mining Claim	18-Jul-22	Active	100
3014617	BAD VERMILION LAKE AREA	298213	Boundary Cell Mining Claim	18-Jul-22	Active	100
3014617	BAD VERMILION LAKE AREA	232199	Single Cell Mining Claim	18-Jul-22	Active	100
855742	BAD VERMILION LAKE AREA	320280	Single Cell Mining Claim	18-Jul-22	Active	100
3014618	BAD VERMILION LAKE AREA	343534	Single Cell Mining Claim	16-Sep-22	Active	100
3014618	BAD VERMILION LAKE AREA	343533	Single Cell Mining Claim	16-Sep-22	Active	100

3014618	BAD VERMILION LAKE AREA	283897	Single Cell Mining Claim	16-Sep-22	Active	100
855726	BAD VERMILION LAKE AREA	315091	Single Cell Mining Claim	9-Dec-22	Active	100
855726	BAD VERMILION LAKE AREA	201842	Single Cell Mining Claim	9-Dec-22	Active	100
855728	BAD VERMILION LAKE AREA	297963	Single Cell Mining Claim	9-Dec-22	Active	100
855728	BAD VERMILION LAKE AREA	279269	Single Cell Mining Claim	9-Dec-22	Active	100
855730	BAD VERMILION LAKE AREA	223246	Single Cell Mining Claim	9-Dec-22	Active	100
855730	BAD VERMILION LAKE AREA	105924	Single Cell Mining Claim	9-Dec-22	Active	100
1240294	BAD VERMILION LAKE AREA	339878	Boundary Cell Mining Claim	2-Jan-23	Active	100
1240294	BAD VERMILION LAKE AREA	339876	Boundary Cell Mining Claim	2-Jan-23	Active	100
1240294	BAD VERMILION LAKE AREA	178359	Boundary Cell Mining Claim	2-Jan-23	Active	100
1240294	BAD VERMILION LAKE AREA	339877	Single Cell Mining Claim	2-Jan-23	Active	100
1240294	BAD VERMILION LAKE AREA	280924	Single Cell Mining Claim	2-Jan-23	Active	100
1240294	BAD VERMILION LAKE AREA	260881	Single Cell Mining Claim	2-Jan-23	Active	100
1240294	BAD VERMILION LAKE AREA	212904	Single Cell Mining Claim	2-Jan-23	Active	100
1240294	BAD VERMILION LAKE AREA	159495	Single Cell Mining Claim	2-Jan-23	Active	100
	LITTLE TURTLE LAKE AREA	631577	Single Cell Mining Claim	20-Jan-23	Active	100
3000810	BAD VERMILION LAKE AREA	328166	Boundary Cell Mining Claim	13-Feb-23	Active	100
3000810	BAD VERMILION LAKE AREA,LITTLE TURTLE LAKE AREA	213563	Boundary Cell Mining Claim	13-Feb-23	Active	100
3000810	BAD VERMILION LAKE AREA	165646	Single Cell Mining Claim	13-Feb-23	Active	100
3014626	BAD VERMILION LAKE AREA	333556	Boundary Cell Mining Claim	13-Feb-23	Active	100
3014626	BAD VERMILION LAKE AREA,LITTLE TURTLE LAKE AREA	319258	Boundary Cell Mining Claim	13-Feb-23	Active	100
3014626	BAD VERMILION LAKE AREA,LITTLE TURTLE LAKE AREA	284821	Boundary Cell Mining Claim	13-Feb-23	Active	100
3014626	BAD VERMILION LAKE AREA	272169	Boundary Cell Mining Claim	13-Feb-23	Active	100
3014626	BAD VERMILION LAKE AREA,LITTLE TURTLE LAKE AREA	235455	Boundary Cell Mining Claim	13-Feb-23	Active	100
3014626	BAD VERMILION LAKE AREA	218294	Boundary Cell Mining Claim	13-Feb-23	Active	100
3014626	BAD VERMILION LAKE AREA	198177	Boundary Cell Mining Claim	13-Feb-23	Active	100
3014626	BAD VERMILION LAKE AREA,LITTLE TURTLE LAKE AREA	169415	Boundary Cell Mining Claim	13-Feb-23	Active	100
3014626	BAD VERMILION LAKE AREA	333555	Single Cell Mining Claim	13-Feb-23	Active	100
3014626	BAD VERMILION LAKE AREA	206162	Single Cell Mining Claim	13-Feb-23	Active	100
3014629	BAD VERMILION LAKE AREA	340968	Single Cell Mining Claim	13-Feb-23	Active	100
3014629	BAD VERMILION LAKE AREA	275877	Single Cell Mining Claim	13-Feb-23	Active	100
3014629	BAD VERMILION LAKE AREA	257440	Single Cell Mining Claim	13-Feb-23	Active	100
3014629	BAD VERMILION LAKE AREA	257439	Single Cell Mining Claim	13-Feb-23	Active	100
3014629	BAD VERMILION LAKE AREA	257438	Single Cell Mining Claim	13-Feb-23	Active	100
3014629	BAD VERMILION LAKE AREA	221463	Single Cell Mining Claim	13-Feb-23	Active	100
3014629	BAD VERMILION LAKE AREA	215418	Single Cell Mining Claim	13-Feb-23	Active	100
3014629	BAD VERMILION LAKE AREA	209930	Single Cell Mining Claim	13-Feb-23	Active	100
3014629	BAD VERMILION LAKE AREA	209929	Single Cell Mining Claim	13-Feb-23	Active	100
3014629	BAD VERMILION LAKE AREA	201899	Single Cell Mining Claim	13-Feb-23	Active	100
3014629	BAD VERMILION LAKE AREA	156768	Single Cell Mining Claim	13-Feb-23	Active	100
3014629	BAD VERMILION LAKE AREA	112285	Single Cell Mining Claim	13-Feb-23	Active	100
3014629	BAD VERMILION LAKE AREA	112284	Single Cell Mining Claim	13-Feb-23	Active	100
	BAD VERMILION LAKE AREA	612297	Single Cell Mining Claim	8-Sep-23	Active	100
	BAD VERMILION LAKE AREA	612296	Single Cell Mining Claim	8-Sep-23	Active	100
	BAD VERMILION LAKE AREA	612295	Single Cell Mining Claim	8-Sep-23	Active	100
	BAD VERMILION LAKE AREA	612294	Single Cell Mining Claim	8-Sep-23	Active	100
	BAD VERMILION LAKE AREA	612293	Single Cell Mining Claim	8-Sep-23	Active	100
	BAD VERMILION LAKE AREA	612292	Single Cell Mining Claim	8-Sep-23	Active	100
	BAD VERMILION LAKE AREA	612291	Single Cell Mining Claim	8-Sep-23	Active	100
	BAD VERMILION LAKE AREA	612290	Single Cell Mining Claim	8-Sep-23	Active	100
	BAD VERMILION LAKE AREA	612289	Single Cell Mining Claim	8-Sep-23	Active	100
	BAD VERMILION LAKE AREA	612288	Single Cell Mining Claim	8-Sep-23	Active	100
	BAD VERMILION LAKE AREA	612287	Single Cell Mining Claim	8-Sep-23	Active	100
	BAD VERMILION LAKE AREA	612286	Single Cell Mining Claim	8-Sep-23	Active	100
	BAD VERMILION LAKE AREA	612285	Single Cell Mining Claim	8-Sep-23	Active	100
	BAD VERMILION LAKE AREA	612284	Single Cell Mining Claim	8-Sep-23	Active	100
	BAD VERMILION LAKE AREA	612283	Single Cell Mining Claim	8-Sep-23	Active	100
	BAD VERMILION LAKE AREA	612282	Single Cell Mining Claim	8-Sep-23	Active	100
	BAD VERMILION LAKE AREA	612281	Single Cell Mining Claim	8-Sep-23	Active	100
	BAD VERMILION LAKE AREA	612280	Single Cell Mining Claim	8-Sep-23	Active	100
	BAD VERMILION LAKE AREA	612279	Single Cell Mining Claim	8-Sep-23	Active	100

BAD VERMILION LAKE AREA	612278	Single Cell Mining Claim	8-Sep-23	Active	100
BAD VERMILION LAKE AREA	612277	Single Cell Mining Claim	8-Sep-23	Active	100
BAD VERMILION LAKE AREA	612276	Single Cell Mining Claim	8-Sep-23	Active	100
BAD VERMILION LAKE AREA	612275	Single Cell Mining Claim	8-Sep-23	Active	100
BAD VERMILION LAKE AREA	612274	Single Cell Mining Claim	8-Sep-23	Active	100
BAD VERMILION LAKE AREA,LITTLE TURTLE LAKE AREA	612270	Single Cell Mining Claim	8-Sep-23	Active	100
LITTLE TURTLE LAKE AREA	618562	Single Cell Mining Claim	9-Nov-23	Active	100
LITTLE TURTLE LAKE AREA	618561	Single Cell Mining Claim	9-Nov-23	Active	100
LITTLE TURTLE LAKE AREA	618560	Single Cell Mining Claim	9-Nov-23	Active	100
LITTLE TURTLE LAKE AREA	618559	Single Cell Mining Claim	9-Nov-23	Active	100
BAD VERMILION LAKE AREA,LITTLE TURTLE LAKE AREA	618618	Single Cell Mining Claim	11-Nov-23	Active	100
BAD VERMILION LAKE AREA	618617	Single Cell Mining Claim	11-Nov-23	Active	100
LITTLE TURTLE LAKE AREA	619247	Single Cell Mining Claim	17-Nov-23	Active	100

Table 2 - Patents & Mining Leases

Mining Right Number	Mining Right Type	Rights	Area	Anniversary	Pin	Reference Plan
LEA-107370	Lease	MR+SR	32.856	30-Jun-22	56066-2758(LT)	Pts. 1 & 2, 48R-1661
LEA-107790	Lease	MR+SR	154.53	31-Aug-26	56066-2492(LT)	Pts. 1-3, 48R-2178
LEA-107791	Lease	MR+SR	41.577	30-Sep-26	56066-2494(LT)56066-2495(LT)	Pts. 4-8, 48R-2178
LEA-107792	Lease	MRO	48.991	31-Oct-26	56066-2496(LT)	Pts. 1-3, 48R-2179
LEA-107872	Lease	MR+SR	176.03	30-Jun-27	56066-2498(LT) 56066-2497(LT) 56066-2499(LT)	Pts. 1-17, 48R-2225
LEA-108775	Lease	MR+SR	85.996	31-Jul-32	56066-3072(LT)	Pts. 1-6, 48R-3078
LEA-109390	Lease	MR+SR	181.34	31-May-33	56066-3075(LT)	Pts. 1 & 2, 48R-3112
PAT-9638	Patent	MRO	16.187		56066-3674(LT)	Mining Loc. AD4
PAT-9641	Patent	MR+SR	16.187		56066-2688(LT)	Mining Loc. AL116
PAT-9642	Patent	MR+SR	14.973		56066-2689(LT)	Mining Loc. AL131

Appendix 2 – 2021 Airborne Survey Technical Report (Munro, 2021)

Q-Gold Resources Ltd.

Heli-GT Three-Axis Magnetic Gradiometer Survey

Mine Centre
Ontario, Canada

Operations and Processing Report

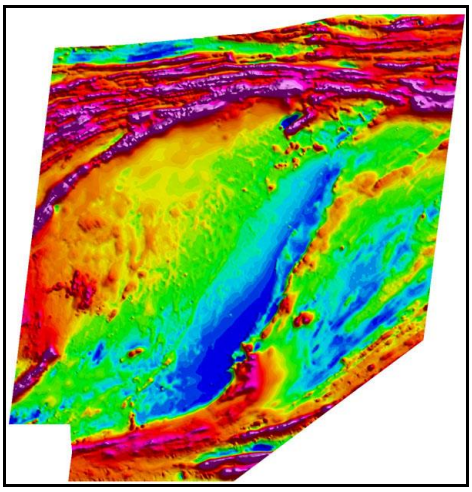

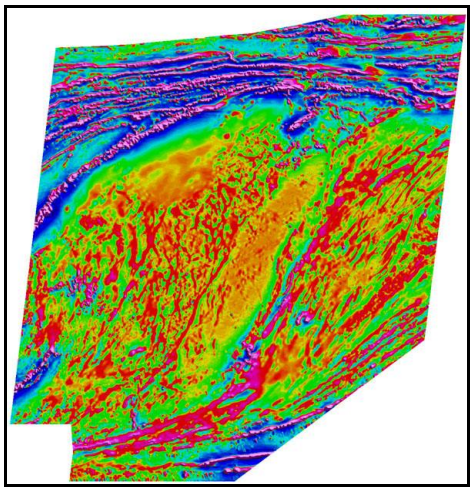

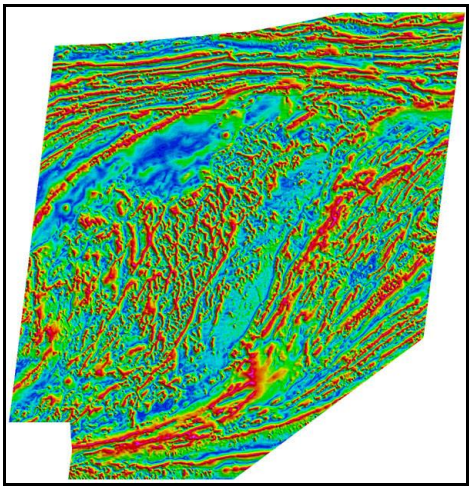

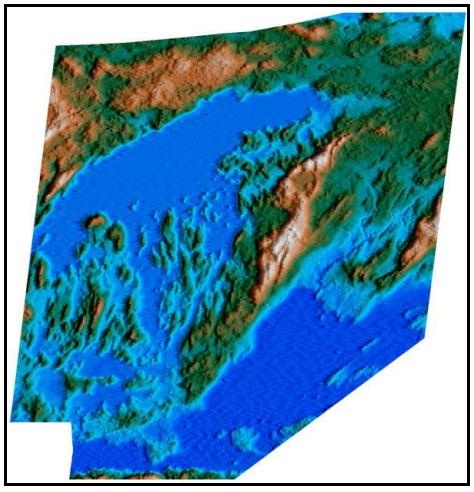

By

SHA GEOPHYSICS LTD

February 17, 2021

TABLE OF CONTENTS

1 INTRODUCTION

In December, 2020 Q-Gold Resources Ltd. (Q-Gold) contracted SHA Geophysics Ltd. (SHA) to carry out a Heli-GT helicopter-towed, three-axis magnetic gradiometer survey over an area of interest surrounding the community of Mine Centre, near Fort Frances, Ontario, Canada. Equipment and crew mobilized to the area on Tuesday, January 19th, 2021 and during the period January 19th to January 30th, 2021 a total of 2575 km of data was collected. Details of the airborne survey and compilation are documented in this report.

2 LOCATION

The survey block was located approximately 50 kilometers east-northeast of the town of Fort Frances, Ontario and approximately 15 kilometers north of the Canada-US border. See Figure 1 below.

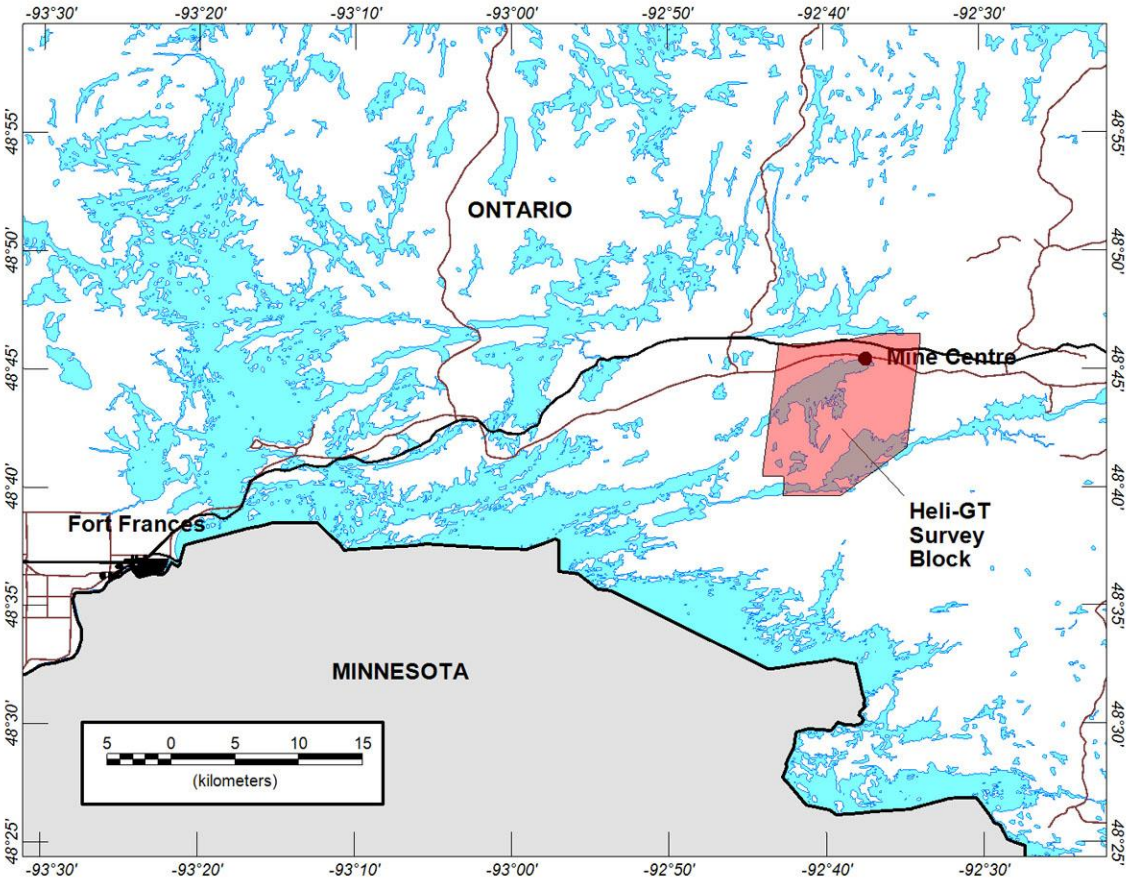

Figure 1 - Location Map.

3 AIRBORNE SURVEY

The survey was based out of a fishing lodge in Mine Centre, Ontario. The lodge was located within the survey block and was accessible by road. Crew and equipment mobilized to the base of operations on Tuesday, January 19th, 2021. Surveying was conducted during the period January 19th to January 30th, 2021. The following table summarizes flight specifications of the block.

3.1 Flight Specifications

Traverse Direction	90° – 270°
Traverse Spacing	50 m
Control Direction	0° – 180°
Control Spacing	1500m
Terrain Clearance	30m
Block Production	2575 km

3.2 Helicopter

Helicopter Owner / Operator	Expedition Helicopters, Cochrane, Ontario
Helicopter Model	A-Star 350D
Helicopter Registration	C-GXIJ

3.3 Personnel

The following personnel were involved in the survey:

Field

Technical Operations Manager	Frazer Hogg
Project Geophysicist	Steve Munro
Pilot	Joel Breton

Office

Compilation and Reporting	Steve Munro
Project Management	Scott Hogg

4 GEOPHYSICAL SYSTEM

The airborne geophysical Heli-GT system consists of a towed bird that contains all of the geophysical sensors as well as altimeter and GPS antennae. A computer based recording and navigation system is located in the helicopter.

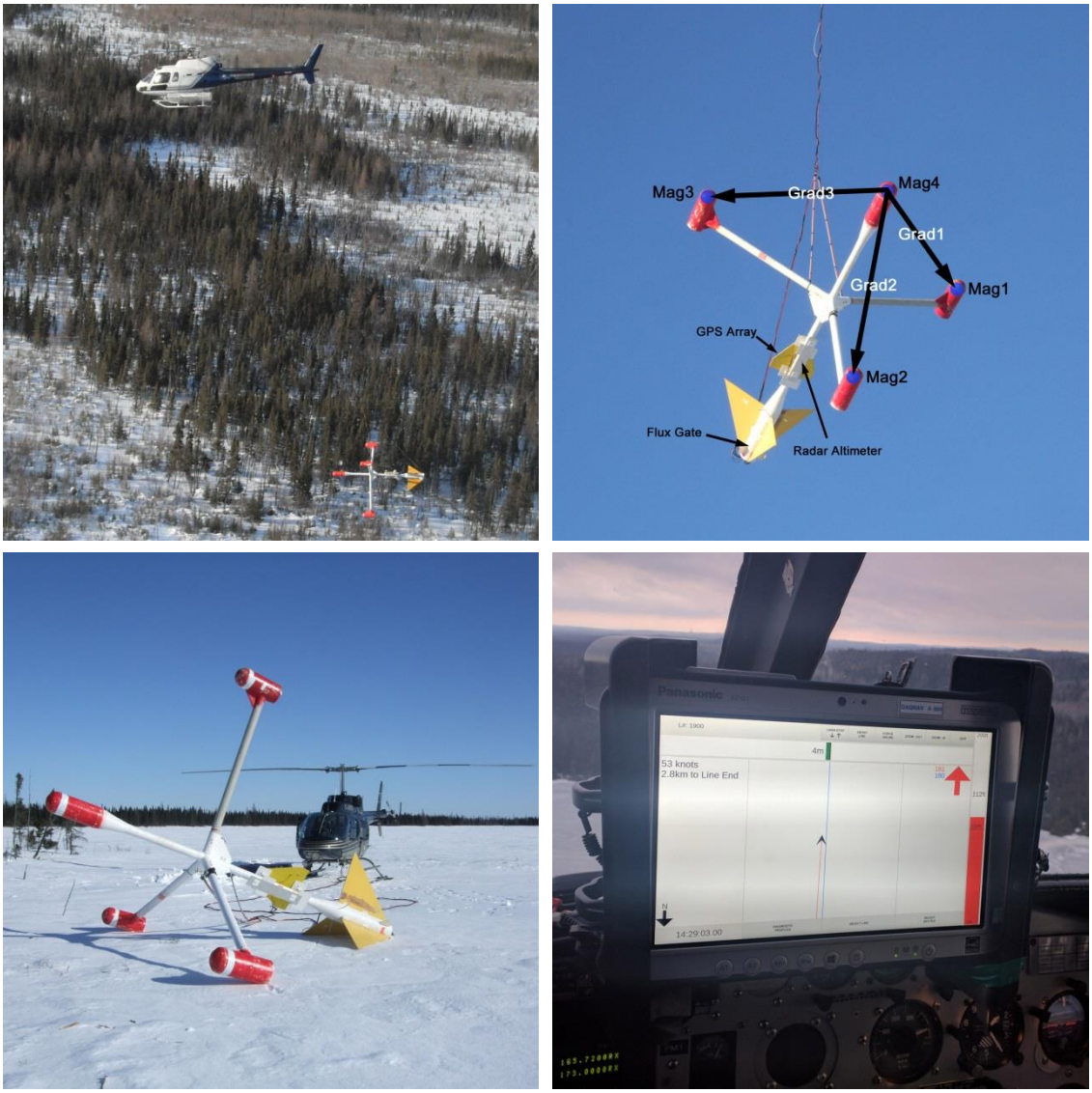

Figure 2 – The Heli-GT bird is towed 25 m below the helicopter. The basic orthogonal magnetic gradients G1, G2 and G3 are measured on 3 metre baselines. A radar altimeter and 4 GPS antennae are mounted on the towed bird. In the helicopter a touch screen computer tablet logs the data and directs navigation.

4.1 Bird

All of the geophysical and ancillary equipment is housed in a towed bird designed by SHA Geophysics Ltd. The bird is manufactured from non-magnetic FRP and breaks down for ease of transportation.

4.2 Magnetic sensors

Four Scintrex CS-3 cesium sensors are arranged in an orthogonal array with 3 m sensor separation from the nose sensor to those at the end of each arm. The output from each sensor was processed by a KVS KMAG4 unit to resolve the magnetometer output to a resolution of about 0.005 nT at a rate of ten samples per second. The Heli-GT bird was flown at a nominal altitude of 30m.

4.3 Radar Altimeter

A Terra TRA 3500 / TR 140 radar altimeter was used to measure bird height above ground. The range of operation was from 0 to 2500 ft.

4.4 Fluxgate Magnetometer

A Billingsley TFM100G2 3-axis fluxgate magnetometer was used to record the orientation of the bird with respect to the earth's magnetic field. The range of each component of the fluxgate was +/- 100,000 nT.

4.5 Analog to Digital ADC

The analog output of the radar altimeter and fluxgate magnetometer were digitized with a KVS KANA8 eight-channel differential ADC. The device provides 24 bit resolution and was operated at 10 Hz.

4.6 GPS System

GPS positional information was recorded using an array of four 12-channel receivers mounted on the Heli-GT bird. In addition to the measurement of Latitude, Longitude and Altitude a calculation of bird pitch, roll and yaw was calculated from differences between antennae with an accuracy better than 1 degree.

4.7 Navigation and Recording System

The navigation and recording system used was the DAQNAV, developed by SHA Geophysics. Both navigation and data recording are carried out using a tablet computer mounted in the helicopter cockpit. The tablet's touch screen provides an operator with an interface for monitoring the geophysical and ancillary instrumentation, as well as presenting graphic navigation information for the pilot.

The PPS pulse from the GPS system was recorded and tied to each of the sensors with an accuracy of about +/- 0.05 seconds.

Data recorded included the following:

Magnetic sensors:	10 Hz
Fluxgate sensors:	10 Hz
Radar Altimeter:	10 Hz
GPS X / Y / Z:	5 Hz
GPS Pitch / roll / yaw:	5 Hz

4.8 Base Station

A magnetic and GPS base station was established at the base of operations. A GEM SSM19TW proton magnetometer recorded the diurnal magnetic variation at 1 Hz with a resolution of 0.1 nT. A Ublox EVK-M8 GPS receiver provided a GPS time reference and recorded a differential correction file.

5 DATA COMPILATION

5.1 Basic Processing

The data collected during flight, in the air and from the base station, was aligned with reference to GPS time. Each of the four magnetometer channels was compensated to remove magnetic error associated with bird orientation. The basic magnetic gradients; G1, G2 and G3, measured from the nose sensor (mag4) to each of the radial sensors (mag1, mag2 and mag3) were calculated. Any noise spikes, if present, were identified and removed.

A low-pass filter was applied to the base station data to eliminate short wavelength artifacts. A median value was removed from the base station profile to create a diurnal correction profile, which was subtracted from the compensated mag4 profile. The base station corrected total field profile was stored as *mag_diur*.

A short lag (0.05 seconds) was applied to the diurnally corrected data. The lagged profile was stored as *mag_lag*.

5.2 Gradient Processing

The recorded pitch, roll and yaw of the bird were used to mathematically rotate the measured basic gradients to true G-north, G-east and G-down.

The GPS altitude of the bird was used to calculate a smooth drape surface. This is a smooth theoretical surface above the terrain that the bird would follow under ideal conditions. There would be only smooth altitude changes, line to line and along the flight line. The difference between the GPS altitude of this smooth drape surface and the actual GPS altitude of the bird was combined with the measured vertical gradient to calculate an altitude correction. The altitude correction was applied to m*ag_lag* and the resulting profile was stored as *mag_alt_cor*.

5.3 Magnetic Levelling

The channel *mag_alt_cor* was used as input to the control line levelling process.

The intersections between traverse and control lines were calculated and the differences between the magnetic values were measured. Ignoring unreliable differences in locations of steep magnetic gradient, a correction was calculated to eliminate the measured differences at the intersections. This correction profile was a piecewise linear function between intersections. The control line leveled magnetic profile was stored as *mag_TL_lev*. A final microlevel correction was calculated and applied. The final data channel was stored as *mag_fin*.

5.4 Gradient Tensor Gridding (GT-GRID)

GT-Grid is a proprietary gridding program developed by SHA Geophysics that uses total magnetic field data as well as the measured horizontal gradient data to produce a total magnetic field grid. The total magnetic field grid produced by GT-Grid is a fully conformal process that simultaneously honours the total field as well as the measured horizontal gradient profile data.

The final, leveled total field magnetic channel (m*ag_fin*) and the G-east (*Ge)* and G-north (*Gn*) gradient channels, were used by the GT-GRID process to calculate a total field magnetic grid.

5.5 Pole Reduction

The anomaly shape associated with a vertically dipping magnetic source varies with the inclination of the earth's magnetic field. At the north and south magnetic pole, the inclination is vertical and the anomaly is positive, symmetrical and centered directly over the source. At the equator, with a horizontal inducing field, the anomaly is negative, symmetrical and centered directly over the source. Between 0 and 90 degrees of inclination the anomaly is asymmetric, with a positive and negative component, and is not centered over the source. The pole reduction process reshapes the anomaly measured at intermediate inclinations to resemble the shape that would have been measured at vertical inclination. Thus a steeply dipping source, without remanent magnetization, would be transformed to a simple positive peak above the source. A pole-reduced TMI grid was calculated.

5.6 First and Second Vertical Magnetic Gradient

The vertical gradient accentuates shorter wavelengths and attenuates longer wavelengths. As a result, the map enhances the anomalies associated with small near-surface magnetic sources while suppressing large-scale regional variations. The vertical gradient presentation provides added visual detail, particularly for small anomalies superimposed on or adjacent to larger anomalies.

The measured or calculated vertical magnetic gradients are also sensitive to the inclination of the earth's magnetic field. In the same manner as the total field, the asymmetry and peak displacement, arising from an inclined field, is removed by the pole reduction process. The horizontal width of the vertical gradient anomaly is about one half of that of the total field anomaly. If the width of the magnetic source is significant, greater than the sensor height above the source, the zero contour of the pole reduced vertical gradient reflects the location of the magnetic contact and the response peak will lie directly above a steeply dipping source.

Using an FFT filter, a pole-reduced first and second vertical derivative grid was created.

5.7 Horizontal Gradient

This is the scalar amplitude of the horizontal gradient vector, calculated from the total magnetic field GT-Grid. The horizontal gradient grid is useful for highlighting geological contacts.

$$HGrad = ((dB/dx)^2 + (dB/dy)^2)^{½}$$

5.8 Analytic Signal

The analytic signal grid presents the scalar magnitude of the full magnetic gradient vector. The analytic signal reflects proximity to the magnetic source, independent of source dip, magnetic field inclination or remanent magnetization.

$$ANS = ((dB/dx)^2 + (dB/dy)^2 + (dB/dz)^2)^{½}$$

5.9 Tilt Derivative Angle

The tilt angle of the magnetic derivative is calculated in radians.

$$TDR = \tan^{-1} [dB/dz / \mathbf{(} (dB/dx)^2 + (dB/dx)^2 \mathbf{)}^{½}]$$

The tilt angle is independent of magnetization and helps emphasize weak anomalies.

5.10 Digital Terrain Model

The digital terrain model was calculated by subtracting the radar altimeter profile from the GPS altitude. Errors in GPS altitude were corrected by microlevelling. The digital terrain was gridded for each survey block using a bi-directional Akima interpolation.

6 DIGITAL DATA ARCHIVE

All of the maps, grids and profile data have been provided in digital form.

6.1 Profile Data

The profile data for the survey block is provided in Geosoft "gdb" format, including the following channels.

Channel	Units	Content
gpstime	seconds	GPS time
X	metres	UTM easting NAD83, Zone 15n
Y	metres	UTM northing NAD83, Zone 15n
lon	degrees	GPS Longitude WGS84
lat	degrees	GPS Latitude WGS84
gpsalt	metres	GPS altitude NAD83
radalt	metres	radar altimeter (bird height)
DTM	Metres	levelled Digital Terrain elevation
fx	nT	Fluxgate axis x (forward)
fy	nT	Fluxgate axis y (port)
fz	nT	Fluxgate axis z (up)
heading	degrees	Bird heading
pitch	degrees	Bird pitch
roll	degrees	Bird roll
basemag	nT	Filtered base station magnetometer
mag1_raw	nT	Raw upper port magnetometer
mag2_raw	nT	Raw down magnetometer
mag3_raw	nT	Raw upper starboard magnetometer
mag4_raw	nT	Raw nose magnetometer
mag1_comp	nT	Compensated upper port magnetometer
mag2_comp	nT	Compensated down magnetometer
mag3_comp	nT	Compensated upper starboard magnetometer
mag4_comp	nT	Compensated nose magnetometer
G1	nT/m	Magnetic gradient: mag4 to mag1
G2	nT/m	Magnetic gradient: mag4 to mag2
G3	nT/m	Magnetic gradient: mag4 to mag3
mag_diur	nT	Base station corrected mag (applied to mag4)
mag_lag	nT	Lagged mag
mag_alt_cor	nT	Altitude-corrected mag
mag_TL_lev	nT	Tie line network leveled mag
mag_fin	nT	Final microlevelled mag
Ge	nT/m	Measured magnetic East gradient
Gn	nT/m	Measured magnetic North gradient
Gv	nT/m	Measured magnetic Vertical gradient

6.2 Gridded Data

The grids, projected in NAD83 UTM Zone 15n coordinates, are in Geosoft format. The cell size is 10 metres. The following is a description of the grid set provided.

Grid Name	Units	Description
Mine_Centre_DTM	metres	Levelled digital terrain model
Mine_Centre_GT-TMI	nT	Total magnetic field GT-Grid
Mine_Centre_GT-TMIRTP	nT	Total magnetic field GT-Grid, reduced to pole
Mine_Centre_GT-CVGRTP	nT/m	Calculated vertical derivative GT-Grid reduced to pole
Mine_Centre_GT-2VGRTP	nT/m^2	Second vertical derivative GT-Grid reduced to pole
Mine_Centre_GT-HGrad	nT/m	Total horizontal magnetic gradient
Mine_Centre_GT-ANS	nT/m	Analytic Signal
Mine_Centre_GT-Tdr	radians	Tilt derivative angle.

GeoTIFF image files (with pixel size of 2m) are also included for each grid type.

6.3 Map Files

Geosoft format maps for each of the grid types have been prepared. The maps are presented at a scale of 1:20,000, in a NAD83, UTM Zone 15n projection.

Map Name	Units	Description
Mine_Centre_DTM	metres	Levelled digital terrain model
Mine_Centre_GT-TMI	nT	Total magnetic field GT-Grid
Mine_Centre_GT-TMIRTP	nT	Total magnetic field GT-Grid, reduced to pole
Mine_Centre_GT-CVGRTP	nT/m	Calculated vertical derivative GT-Grid reduced to pole
Mine_Centre_GT-2VGRTP	nT/m^2	Second vertical derivative GT-Grid reduced to pole
Mine_Centre_GT-HGrad	nT/m	Total horizontal magnetic gradient
Mine_Centre_GT-ANS	nT/m	Analytic Signal
Mine_Centre_GT-TDR	Radians	Tilt derivative angle.

Corresponding sets of JPEG and PDF images (at a resolution of 200 dpi) are also included.

Respectfully submitted,

Steve Munro, P.Geo (limited)
Chief Geophysicist
SHA Geophysics Ltd.
Toronto, Canada
February 17, 2021